

JAERI-M

放射性同位体製造資料-1244

8450

DETERMINATION OF PLUTONIUM ISOTOPIC RATIOS  
BY Ge(Li)  $\gamma$ -RAY SPECTROMETRY

September 1979

Hiroshi BABA, Toshio SUZUKI, Yoshinori NAKAHARA,  
Hideyuki YAGI and Shuji OKAZAKI

日本原子力研究所  
Japan Atomic Energy Research Institute

この報告書は、日本原子力研究所が JAERI-M レポートとして、不定期に刊行している研究報告書です。入手、複製などのお問い合わせは、日本原子力研究所技術情報部（茨城県那珂郡東海村）あて、お申しこしてください。

JAERI-M reports, issued irregularly, describe the results of research works carried out in JAERI. Inquiries about the availability of reports and their reproduction should be addressed to Division of Technical Information, Japan Atomic Energy Research Institute, Tokai-mura, Naka-gun, Ibaraki-ken, Japan.

Determination of Plutonium Isotopic Ratios  
by Ge(Li)  $\gamma$ -Ray Spectrometry

Hiroshi BABA, Toshio SUZUKI<sup>+</sup>, Yoshinori NAKAHARA<sup>+</sup>,  
Hideyuki YAGI<sup>++</sup>, and Shuji OKAZAKI<sup>+</sup>

Division of Radioisotope Production,  
Radioisotope Center, JAERI

(Received August 28, 1979)

Nondestructive analysis of plutonium was attempted by Ge(Li)  $\gamma$ -ray spectrometry. Gamma-ray spectra were taken by measuring plates of plutonium metal in suppression of the intense low-energy radiation from  $^{241}\text{Am}$  with lead absorber. Twelve complex peak multiplets, each consisting of  $\gamma$  rays from more than one nuclide, were selected from the resulting spectrum in the energy region covering from 200 to 800 keV to determine relative abundances of plutonium isotopes of the mass number from 238 to 241 besides  $^{241}\text{Am}$  etc. Each peak multiplet was unfolded by the usual linear least squares method on the basis of the normalized response profile of each existing nuclide generated with symmetric or asymmetric Gaussians of given energies and relative intensities. The width of Gaussian and the conversion from energy to channel number were self-determined by the non-linear function minimization method. First, the relative abundance of  $^{241}\text{Am}$  with respect to the

---

<sup>+</sup>) Division of Chemistry, Tokai Research Establishment, JAERI

<sup>++</sup>) Division of Reactor Engineering, Tokai Research Establishment, JAERI

content of  $^{239}\text{Pu}$  was obtained by the use of the unfolding results of three particular peak multiplets. Then, contents of the other nuclides relative to the content of  $^{239}\text{Pu}$  were determined with fixing the abundance ratio between  $^{241}\text{Am}$  and  $^{239}\text{Pu}$  to the obtained value in analysis of the remaining multiplets. Finally, the effective detection efficiency curve was constructed with eleven out of the twelve values of  $^{239}\text{Pu}$  abundance plus the peak intensity of one single peak of  $^{239}\text{Pu}$ . The efficiency curve can be used to re-evaluate relative contents of the nuclides observed above. Reliability of the present method shall be discussed with regard to the isotopic grade of plutonium samples and interference due to the existence of fission product nuclides.

Keywords: Ge(Li) Detector,  $\gamma$ -Ray Spectrometry, Plutonium Isotopes, Isotopic Ratio, Nondestructive Analysis, Spectrum Unfolding, Reliability

Ge(Li)  $\gamma$ 線スペクトロメトリによる  
プルトニウム同位体比の決定

日本原子力研究所アイソトープ事業部製造部

馬場 宏・鈴木敏夫<sup>+</sup>・中原嘉則<sup>+</sup>八木秀之<sup>++</sup>・岡崎修二<sup>+</sup>

(1979年8月28日受理)

Ge(Li)  $\gamma$ 線スペクトロメトリによるプルトニウム試料の非破壊分析を試みた。板状の金属プルトニウムを測定試料として、試料中に含まれる<sup>241</sup>Amの強い低エネルギー放射線を鉛吸収板でカットした状態で $\gamma$ 線スペクトルを測定した。得られたスペクトルについて、200 KeVから800 KeV迄のエネルギー範囲を選び、質量数238から241迄のプルトニウム同位元素や<sup>241</sup>Am等の核種の存在比を求めるのに適当な13個のピーク群を設定した。これらのピーク群は、1個を除いていずれも2個以上の核種からの $\gamma$ 線群によって構成されている。各ピーク群は、その寄与する核種毎に既知のエネルギーと存在比の値を使って純粋なスペクトルを合成し、次に規準化した純粋スペクトルとして通常の線型最小自乗法によるフィッティングを行うことにより解析した。核種毎の強度は、その際に得られた規準化スペクトルにかゝる振幅係数によって定められる。ただし、各 $\gamma$ 線の応答関数は対称又は非対称ガウス曲線で表わし、ガウス曲線の巾とエネルギー対チャンネル数の変換係数は非線型関数値最小化法によって定めた。

最初に、特定の3つのピーク群から<sup>241</sup>Am/<sup>239</sup>Puが求まり、次にこうして定めた<sup>241</sup>Am/<sup>239</sup>Puの値を用いて残りのピーク群の解析を行い、他の核種についての相対存在比を求めた。最後に、これら12個の複合ピーク群のうちの11個のピーク群の解析から得られた<sup>239</sup>Puの相対存在量と別に1個の単一ピークから求めた<sup>239</sup>Puの存在量の合わせて12個の値を用いて実質的な検出効率曲線を作成した。この検出効率曲線を用いて、必要ならば、上述のピーク群の解析結果の再評価を行うことも出来る。

現解析法の信頼性を<sup>239</sup>Puの純度や核分裂生成物の混合状態等との関連において論じる。

---

+ ) 東海研究所原子炉化学部

++ ) 東海研究所原子炉工学部

Contents

1. Introduction .....	1
2. Experimental .....	4
3. Analyzing Program PASAY .....	6
4. Results and Discussion.....	9
References .....	17
Tables .....	18
Figures .....	27

## 目 次

1. 序 論 .....	1
2. 実 験 .....	4
3. 解析プログラム PASAY .....	6
4. 結果と考察 .....	9
文 献 .....	17
表 .....	18
図 .....	27

## 1. Introduction

Accurate determination of the isotopic ratios of plutonium samples has recently been attempted by means of high-resolution  $\gamma$ -ray spectrometry from the view point of the plutonium fuel assessment<sup>1-3)</sup>. Plutonium samples as isotopic mixture generally contain decay products such as  $^{241}\text{Am}$ ,  $^{228}\text{Th}$ , and the fission products from the fissile plutonium. Of those decay products,  $^{241}\text{Am}$  causes the most serious trouble for the high-resolution  $\gamma$ -ray spectrometry of plutonium samples because of its tremendously intense 59-keV  $\gamma$ -ray among other  $\gamma$  rays.

There are two ways to perform plutonium assay with the Ge(Li) spectrometry. Gunnink has attempted to utilize the X-ray spectra<sup>3)</sup>, in which one can reduce to some extent the interference of the huge 59-keV  $\gamma$  ray from  $^{241}\text{Am}$ . However, one encounters another difficulty in the X-ray spectrometry that the X-ray response profile is of broadened shape<sup>4)</sup> different from that of  $\gamma$  rays and there exist many satellite peaks locating so closely to each other that the unfolding of the spectrum is too difficult to assure a reliable result.

An alternative method of the plutonium determination is to suppress the low-energy  $\gamma$  rays and X rays with thick absorber, so that one can measure high-energy  $\gamma$  rays of extremely weak intensities without any pile-up distortion.

There is an additional problem to be solved when one tries to apply the above high-resolution  $\gamma$ -ray spectrometry to the non-destructive determination of the plutonium isotopic ratios. It is the uncertainty in the counting efficiency and



$\gamma$ -ray attenuation by the sample matrix or other absorbing materials. Non-uniform package or inhomogeneity of the sample would result in a significantly different counting condition for every measurement of each sample.

As it has been pointed out by Gunnink<sup>5)</sup>, the above difficulty can, however, be removed to a considerable degree by grouping appropriate neighbouring peaks in the obtained spectrum to compute the isotopic ratios from the observed peak intensities. By this technique, one can assure the least errors introduced due to the differences in the detection efficiency and the attenuation factors among the involved peaks.

One picks up certain peak multiplets consisting of  $\gamma$  rays from more than one nuclide in the obtained spectrum. The unfolding procedure is based on the usual linear least squares fit, in principle, using the normalized response profile constructed for each nuclide by the use of the known energies and intensities of the relevant  $\gamma$  rays. The resulting normalization factors give relative abundances among the involved nuclides and, if one knows the absolute detection efficiency, the absolute numbers of atoms can also be deduced.

Gunnink shows that he can obtain very accurate isotopic ratios of plutonium by the above-mentioned  $\gamma$ -ray spectrometry in the case of plutonium samples of high purity, i.e. of very low  $^{241}\text{Am}$  content and with no fission products<sup>5)</sup>. Gunnink's study has, however, been performed under an ideal condition. In the routine work, one must treat a large number of samples with various types of history under much more severe counting

conditions. The resulting spectrum would be of rather poor statistics and the counting condition would not precisely be reproduced from sample to sample.

We have carried out a field experiment of Ge(Li)  $\gamma$ -ray spectrometry of plutonium samples of various grades for finding an optimum experimental set-up. Then we attempted to establish an algorithm of complete self-determination of the plutonium isotopic ratios by the use of thus obtained  $\gamma$ -ray spectra. The present work mainly concerns the latter; namely, the construction of the algorithm and its feasibility study with non-idealized plutonium samples.

## 2. Experimental

Figure 1 shows a schematic view of the counting set-up for the non-destructive analysis of plutonium. The sample was placed at 40cm apart from the detector surface. As the detector, two Ge(Li) detectors were used; one with 6.6% efficiency and 2.1 keV resolution and the other with 12.6% efficiency and 2.2 keV resolution. The specimens were plutonium metal plates aged for about 10 years. Three sizes of the specimens were used as the counting sample, namely, 1"x4"x1/16", 2"x4"x1/16", and 4"x4"x1/16", respectively. Plutonium samples measured were parted in three groups with respect to the isotopic grade; namely, 92%, 81%, and 75% for  $^{239}\text{Pu}$ .

A lead absorber of 2mm thick was placed just below the sample in order to attenuate the strong 59-keV  $\gamma$ -ray of  $^{241}\text{Am}$  and X rays. A thin lead absorber and a cadmium absorber were also inserted just above the detector surface, the former cut the scattered  $\gamma$  rays while the latter absorbed the lead fluorescent X ray.

More than 40 measurements were carried out with the above set-up, most of which were performed without the effect of the pile-up rejector. Figure 2 shows a typical example of the  $\gamma$ -ray spectrum obtained. Here, the channel number in the abscissa corresponds to four times the energy. One may recognize that the sample contained significant amounts of  $^{241}\text{Am}$  and fission products which were accumulated during the experiments at the Fast Critical Assembly of JAERI. Low energy portion of the spectrum was strongly attenuated with the thick lead absorber.

The total count rate was suppressed below 5,000 cps for avoiding pile-up distortion because most were undertaken without pile-up rejector. Furthermore, the duration of each measurement was restrained to 4 kiloseconds under the speculation of a practicable on-site working condition.

### 3. Analyzing Program PASAY

Thirteen peak multiplets were selected for determining isotopic ratios of plutonium, which are designated with Roman numerals from II to XIV in Fig.3 and listed in Table 1. The peak grouping I almost disappeared in the present counting condition, so that it was not used in the present work though it is important in the analysis of pure plutonium samples.

Twelve of the above thirteen peak complexes consists of  $\gamma$  rays from two or more nuclides, while the peak group VII is a single peak of the 451.5-keV  $\gamma$  ray from  $^{239}\text{Pu}$ . The groupings coloured in red were of particular importance in the isotopic ratio determination.

The principle of the analysis is similar to that discussed by Gunnink<sup>5)</sup>. First, the energy calibration curve was constructed with the twelve prominent peaks pointed in Fig.3. Next, large peaks or peak compounds in the spectrum are picked up and their widths are extracted by the non-linear least squares fit following the algorithm of a  $\gamma$ -ray spectrum analyzing program BOB73<sup>8)</sup>. Then the relationship between the peak width and energy is obtained with thus found values of the peakwidth and channel, and the energy calibration curve.

Now, each peak multiplet was unfolded by the usual linear least squares method on the basis of the normalized response profile of each existing nuclide that was generated with symmetric or asymmetric Gaussians of given energies and intensities<sup>6,7)</sup>. Here, the width of the Gaussian and the conversion from energy to channel number were self-determined by the non-linear function minimizing method<sup>9)</sup>.

In the unfolding of peak groupings, evaluation of the background continuum under the peaks was the most critical factor as discussed elsewhere<sup>10)</sup>. We have used for most peak groupings background continua formed by superimposed step functions, each of which was associated with the relevant peak in its position and relative intensity; namely, the background function  $\underline{B}(x)$  is given by<sup>8)</sup>

$$\underline{B}(x) = (\underline{h}_2 - \underline{h}_1) \frac{\sum_{j=1}^k \underline{p}_j \underline{S}(x - \underline{x}_0^j)}{\sum_{i=1}^k \underline{p}_i} + \underline{h}_1, \quad (1)$$

where  $\underline{h}_1$  and  $\underline{h}_2$  are the counts at the boundaries of the grouping in the low- and high-energy sides,  $\underline{p}_j$  is the height of the  $j$ th peak among  $k$  prominent peaks in the grouping, and  $\underline{x}_0^j$  is the peak channel of the  $j$ th prominent peak.  $\underline{S}$  is a sharp step function defined by

$$\underline{S}(x) = \begin{cases} 0 & \text{for } x < 0 \\ 0.5 & \text{for } x = 0 \\ 1.0 & \text{for } x > 0. \end{cases} \quad (2)$$

As an exceptional case, a simple exponential curve was used as the background for group IX, with consideration of the neighbouring Compton continuum.

The relative abundance of  $^{241}\text{Am}$  with respect to the content of  $^{239}\text{Pu}$  was obtained by the use of the unfolding results of three peak groupings, IV, V, and VI. The relative content of  $^{241}\text{Pu}$  was determined at the same time in the cases of groups IV and V. Contents of the other nuclides were determined relative to the content of  $^{239}\text{Pu}$  with fixing the isotopic ratio between  $^{241}\text{Am}$  and  $^{239}\text{Pu}$  to the obtained value, in the unfolding of other peak groupings. The relative con-

tent of  $^{240}\text{Pu}$  was obtained with groups IX and XI, while that of  $^{238}\text{Pu}$  was found with groups XIII and XIV. Some decay products were also able to be determined with appropriate peak groupings.

Finally, the effective detection efficiency curve was constructed with the values of the  $^{239}\text{Pu}$  content obtained with twelve peak groupings through II to XIII, which could be used, if necessary, for re-evaluation of the relative contents among the nuclides observed above.

#### 4. Results and Discussion

Figures through 4 to 14 exemplify typical unfolding results for various peak groupings under different situations. Observed data after being smoothed are depicted with solid circles, while the black solid curve gives calculated spectra together with an appropriately taken background continuum plotted with the dotted line. The  $\gamma$ -ray spectrum to be attributed to each nuclide is displayed with a coloured curve.

Figures 4a and 4b represent the results of the analyses with the group IV for a 92% and a 75%  $^{239}\text{Pu}$  sample, respectively. The group IV turned out to be a very important peak multiplet for its various advantages. First of all, the count rate in this region is relatively high and, therefore, one can obtain rather good statistics. Secondly, no fission product nuclide feeds prominent  $\gamma$  rays interfering the unfolding of the multiplet.

Thirdly, the  $\gamma$  rays of the involved three nuclides possess more or less comparable intensities to each other so that the least squares analysis is expected to be fairly accurate for a wide range of the isotopic grade of  $^{239}\text{Pu}$ . That is, the abundance of  $^{239}\text{Pu}$  can be independently found from the right-half portion of the multiplet, and then the contents of  $^{241}\text{Pu}$  and  $^{241}\text{Am}$  are determined from the residue of the left-half portion subtracted by the contribution of the  $^{239}\text{Pu}$   $\gamma$  rays, as shown in Figs.4. Moreover, it is obviously seen that the minor fluctuation in the background continuum little affects the result of the analysis.



According to the above procedure of the analysis, the error involved in the content of  $^{239}\text{Pu}$  consists of the statistical error and the uncertainty in the background continuum. On the other hand, the errors in the contents of  $^{241}\text{Pu}$  and  $^{241}\text{Am}$  contain the error in the evaluated contribution of  $^{239}\text{Pu}$  in the left-half fitting region besides the above two sources of error.

The group V consists of the  $\gamma$  rays from the same three nuclides as the group IV does. Moreover, the situation is similar concerning relatively good statistics and little interference of the fission product nuclides. However, there is one important difference between the groups IV and V, as being seen in Figs.5. Namely, all  $\gamma$  rays of  $^{241}\text{Am}$  in this region are masked by anyone of the  $\gamma$  rays of  $^{239}\text{Pu}$  or  $^{241}\text{Pu}$ . As a consequence, the determining 368.6-keV  $\gamma$  ray for  $^{241}\text{Am}$  is greatly affected even by minor misadjustment of the background continuum, particularly in the case of the 92% samples (cf. Fig.5a). Overestimation of the background results in the underestimation of the 368.6-keV peak intensity and vice versa. On the contrary, the content of  $^{241}\text{Pu}$  is expected to be determined with sufficient accuracy indifferent to the isotopic grade or the degree of the correctness of background. This can be seen in Table 2, in which the determined isotopic ratios are compared with those obtained by the mass spectrometric method. Estimation of the attached error was carried out in the same manner as in the case of group IV.

The group VI consists of the  $\gamma$  rays of  $^{239}\text{Pu}$  and  $^{241}\text{Am}$  only, and their contents can be determined with more or less

equal weights as seen in Figs.6. The two advantages of good statistics and little interference of fission product nuclides still remain with this grouping.

The group IX consists of  $\gamma$  rays from three nuclides  $^{239}\text{Pu}$ ,  $^{241}\text{Am}$ , and  $^{240}\text{Pu}$ . Therefore, it is used for determining the isotopic ratio between  $^{240}\text{Pu}$  and  $^{239}\text{Pu}$  using the previously found  $^{241}\text{Am}/^{239}\text{Pu}$  ratio. Unfortunately, the statistics is relatively poor in this region and the branching ratio of the 642.5-keV  $^{240}\text{Pu}$   $\gamma$  ray is fairly small as shown in Figs.7, so that the error due to the background fluctuation and the statistical error in the above-mentioned peak area is of considerable magnitude as indicated in Table 2. This is the reason why the accurate determination of the fissile-to-total plutonium ratio is difficult by  $\gamma$  spectrometry alone.

There are alternative peak groupings for determining the  $^{240}\text{Pu}$  content. One is in the energy region from 160 to 166 keV, which is denoted as the group I in Figs.3. Under our present experimental condition, the  $\gamma$  attenuation was so large in this region that the peak grouping was hardly usable.

One may improve the situation to some extent by reducing the thickness of absorber to be used and avoiding the pile-up distortion using the pile-up rejector. Even so, one must still suffer from the sharp energy dependence of the effective detection efficiency in this region. This would in turn result in rather large error in the unfolding result.

The other peak grouping for  $^{240}\text{Pu}$  covers the energy range from 684 to 711 keV. This is named group XI. There appears the 696-keV  $\gamma$  ray of  $^{144}\text{Ce}$ , though it is not much interfering

the analysis, besides  $\gamma$  rays from three other nuclides,  $^{239}\text{Pu}$ ,  $^{241}\text{Am}$ , and  $^{240}\text{Pu}$ . Shortages of this grouping for determining the  $^{240}\text{Pu}/^{239}\text{Pu}$  ratio are that the statistics is rather poor in this region and that the 688-keV peak of  $^{240}\text{Pu}$  is almost completely masked by the 689-keV peak of  $^{239}\text{Pu}$  as shown in Figs.8. Therefore, one can hardly expect a better result with group XI compared to that with group IX.

The group XII gives information on the relative amount of  $^{228}\text{Th}$ , the decay product from  $^{232}\text{U}$  or  $^{236}\text{Pu}$ . Here, the  $^{241}\text{Am}/^{239}\text{Pu}$  ratio must be known. Existence of the fission products results in the appearance of the 724-keV  $\gamma$  ray of  $^{95}\text{Zr}$  in this region (cf. Figs.9). Then, four nuclides,  $^{239}\text{Pu}$ ,  $^{241}\text{Am}$ ,  $^{228}\text{Th}$ , and  $^{95}\text{Zr}$ , contribute this grouping. As seen from Figs.9, determination of relative abundances of  $^{228}\text{Th}$  and  $^{95}\text{Zr}$  may not be very difficult in spite of the rather poor statistics.

The information on  $^{228}\text{Th}$  can be independently obtained with group XIII, in which one recognizes at most five nuclides as shown in Figs.10. However, the 763-keV  $\gamma$  ray of  $^{228}\text{Th}$  is weak and, in the case of high-grade sample (92%), scarcely distinct out of the background line. Consequently, the obtained  $^{228}\text{Th}/^{239}\text{Pu}$  ratio is considered less reliable compared to that determined with group XII.

The group XIII also supplies two other isotopic ratios,  $^{95}\text{Zr}/^{239}\text{Pu}$  and  $^{238}\text{Pu}/^{239}\text{Pu}$ . As for  $^{95}\text{Zr}$ , there appear one  $\gamma$  ray from  $^{95}\text{Zr}$  (757 keV) and one from its daughter  $^{95}\text{Nb}$  (766 keV). We can say that the determined isotopic ratio would be sufficiently accurate for samples containing so much amount of

$^{95}\text{Zr}$  as to letting the above  $\gamma$  peaks be prominent.

Accurate determination of the  $^{238}\text{Pu}/^{239}\text{Pu}$  ratio is not always easy since  $^{238}\text{Pu}$  is a minor component. As seen from Figs.10, the 766-keV peak of  $^{238}\text{Pu}$  is strongly affected by the existence of the  $^{95}\text{Nb}$  766-keV  $\gamma$  ray. Furthermore, the least squares fit does not seem satisfactory, particularly in the case of the 92% sample of low FP content (cf. Fig.10a). This suggests that either  $\gamma$  ray data used are not correct or some  $\gamma$  rays are overlooked in this peak grouping, for the above misfit does not seem being caused merely by the incorrectness in the background continuum.

A doublet between 735 and 745 keV consists of two  $\gamma$  rays, one emitted from  $^{241}\text{Am}$  and the other from  $^{238}\text{Pu}$ . This doublet named group XIV is also utilized for determination of the  $^{238}\text{Pu}/^{239}\text{Pu}$  ratio. This doublet is not much disturbed by the FP  $\gamma$  rays, but unfortunately the statistics becomes very poor and the peaks are very small particularly for high-grade plutonium samples, as shown in Figs.3 and 11. Which grouping, XIII or XIV, gives more reliable value for the  $^{238}\text{Pu}/^{239}\text{Pu}$  ratio is a rather difficult question at present. One may need more systematic experiment or an appropriate simulation work before one can answer this question.

In Table 2, results of the present work are tabulated in comparison with those obtained by the mass-spectrometric method. The errors attached to the present data were evaluated considering the result of the following simulation work<sup>11)</sup>. Fairly large errors are resulted from insufficient statistics of the observed spectra as a whole, which was inevitable

because of the experimental restriction. Anyhow, one may say the two sets of data agree within the error.

There were five other peak groupings playing subsidiary roles. The group II is an apparent doublet consisting of three  $\gamma$  rays, one from each one of the three nuclides,  $^{239}\text{Pu}$ ,  $^{241}\text{Pu}$ , and  $^{241}\text{Am}$  (cf. Fig.12). Therefore, it should be usable for determination of  $^{241}\text{Pu}/^{239}\text{Pu}$  with the known value of  $^{241}\text{Am}/^{239}\text{Pu}$ . However, it turned out to give an obviously higher value than the isotopic ratio obtained with either group IV or V, as shown in Table 2. The background shape defined by Eq.(1) would probably be responsible for the discrepancy. The desirable shape of the background is likely of an intermediate shape between the superposition of step functions and a simple exponential curve. As a consequence, the group II was used for obtaining the  $^{239}\text{Pu}$  intensity only like other subsidiary groupings.

The group III is apparently a single peak, which actually consists of two  $\gamma$  rays from two nuclides, while group VII is a genuine single peak of  $^{239}\text{Pu}$  alone. The 622-keV  $\gamma$  ray of  $^{106}\text{Ru}$  is contained together with  $\gamma$  rays from  $^{239}\text{Pu}$  and  $^{241}\text{Am}$  in the group XIII, as shown in Figs.13. The group X contains the 662-keV  $\gamma$  ray from  $^{137}\text{Cs}$  as shown in Figs.14. These two groupings, therefore, supply the relative abundances of the fission product nuclides.

Quantitatively speaking, the least squares fit is generally satisfactory throughout Figs.4 to 14, except for some cases of the group VIII as stated before and for the group XI. Disagreement between the observed and fitted spectrum profiles

is consistently observed in the 709-keV peak of  $^{241}\text{Am}$  in the case of group XI. This suggests that the given intensity of the above  $\gamma$  ray is not correct; if this speculation is right, the true intensity should be larger than  $6.41 \times 10^{-8}$  by 20 to 30 percent. However, this peak does not play an important role in the least squares analysis as shown in Figs.8, so that the change in the intensity scarcely affects the deduced isotopic ratios. There might be some other discrepancies in the fit of group XI. They are, however, all trivial considering that the large fluctuations in the spectrum.

Banham discusses reliability of the  $\gamma$  ray data used in the  $\gamma$ -spectrometric determination of plutonium isotopic ratios, and proposes a modified set of the  $\gamma$  data coupled with his analyzing method<sup>12)</sup>. In connection with the present work, we note with particular interest Banham's data set for the intensities of the  $\gamma$  rays belonging to the group II; namely,  $5.70 \times 10^{-7}$  for the  $^{239}\text{Pu}$  203-keV,  $5.6 \times 10^{-6}$  for the  $^{241}\text{Pu}$  208-keV, and  $7.6 \times 10^{-6}$  for the  $^{241}\text{Am}$  208-keV  $\gamma$  rays (cf. Table 1). It is true that with the above  $\gamma$  data set we can obtain the  $^{241}\text{Pu}/^{239}\text{Pu}$  ratio in good agreement with that deduced from the group IV. However, we feel that one must carefully study the  $\gamma$ -ray spectra of pure sources of these isotopes before one make the final decision on the  $\gamma$  data.

With this reservation, the  $\gamma$ -ray data given by Gunnink<sup>6)</sup> may be concluded to work satisfactorily for the isotopic ratio determination.

The presently developed analyzing method was applied to 63 spectrum data obtained with samples of three grades, 92%,

82%, and 75% fissile plutonium contents. The results are shown in Figs.16, in which the observed contents are plotted with solid circles accompanying the error bar in comparison with the book values depicted with open circles. The deduced content agrees with the book value within the evaluated error, except for a few cases.

## References

1. R.Gunnink, J.B.Niday, and P.D.Siemens, UCRL-51577 Pt.1 (1974).
2. T.N.Dragnev, J. Radioanal. Chem. 36 (1977) 491.
3. R.Gunnink, UCRL-80464 (1978).
4. R.Gunnink, Nucl. Instr. and Methods 143 (1977) 145.
5. R.Gunnink, UCRL-51605 (1974).
6. R.Gunnink, J.E.Evans, and A.L.Prindle, UCRL-52139 (1976).
7. W.W.Bowman and K.W.MacMurdo, Atomic Data and Nuclear Data Tables, Vol.13, Nos.2-3 (1974).
8. T.Shimanouchi and I.Suzuki, J. Chem. Phys. 42 (1965) 296.
9. H.Baba, T.Sekine, S.Baba, and H.Okashita, JAERI 1227 (1973).
10. H.Baba, S.Baba, and T.Suzuki, Nucl. Instr. and Methods 145 (1977) 517.
11. H.Baba and H.Yagi, JAERI-M 8451 (1979).
12. M.F.Banham, AERE-R 8737 (1977).





Table 1. (continued)

Source	Energy (keV)	Intensity	Reference	Source	Energy (keV)	Intensity	Reference
$^{241}\text{Am}$	376.595	$1.38 \times 10^{-6}$	6	$^{239}\text{Pu}$	617.10	$1.34 \times 10^{-8}$	6
$^{239}\text{Pu}$	380.166	$3.05 \times 10^{-6}$	6	$^{239}\text{Pu}$	618.28	$2.04 \times 10^{-8}$	6
$^{239}\text{Pu}$	382.751	$2.59 \times 10^{-6}$	6	$^{241}\text{Am}$	619.00	$5.94 \times 10^{-7}$	6
$^{241}\text{Am}$	383.74	$2.82 \times 10^{-7}$	6	$^{239}\text{Pu}$	619.21	$1.21 \times 10^{-8}$	6
				$^{106}\text{Ru}$	621.8	$9.76 \times 10^{-2}$	7
	<u>Group VI (409.0 - 431.0 keV)</u>				<u>Group IX (630.0 - 649.0 keV)</u>		
$^{239}\text{Pu}$	411.15	$6.8 \times 10^{-8}$	6	$^{241}\text{Am}$	633.0	$1.26 \times 10^{-8}$	6
$^{239}\text{Pu}$	413.712	$1.489 \times 10^{-5}$	6	$^{239}\text{Pu}$	633.15	$2.53 \times 10^{-8}$	6
$^{241}\text{Am}$	419.24	$2.87 \times 10^{-7}$	6	$^{239}\text{Pu}$	637.837	$2.56 \times 10^{-8}$	6
$^{239}\text{Pu}$	422.586	$1.193 \times 10^{-6}$	6	$^{239}\text{Pu}$	640.075	$8.20 \times 10^{-8}$	6
$^{241}\text{Am}$	426.39	$2.46 \times 10^{-7}$	6	$^{241}\text{Am}$	641.42	$7.10 \times 10^{-8}$	6
$^{239}\text{Pu}$	426.68	$2.328 \times 10^{-7}$	6	$^{240}\text{Pu}$	642.48	$1.245 \times 10^{-7}$	6
$^{239}\text{Pu}$	428.4	$1.00 \times 10^{-8}$	6	$^{239}\text{Pu}$	645.969	$1.489 \times 10^{-7}$	6
$^{241}\text{Am}$	429.84	$1.15 \times 10^{-8}$	6				
$^{239}\text{Pu}$	430.08	$4.30 \times 10^{-8}$	6				
					<u>Group X (649.0 - 665.5 keV)</u>		
	<u>Group VII (448.5 - 453.5 keV)</u>			$^{239}\text{Pu}$	649.321	$7.12 \times 10^{-9}$	6
$^{239}\text{Pu}$	451.474	$1.89 \times 10^{-6}$	6	$^{239}\text{Pu}$	650.529	$2.70 \times 10^{-9}$	6
				$^{239}\text{Pu}$	652.074	$6.55 \times 10^{-8}$	6
	<u>Group VIII (615.5 - 623.5 keV)</u>			$^{241}\text{Am}$	652.96	$3.77 \times 10^{-7}$	6

Table 1. (continued)

Source	Energy (keV)	Intensity	Reference	Source	Energy (keV)	Intensity	Reference
$^{239}\text{Pu}$	654.880	$2.25 \times 10^{-8}$	6	$^{239}\text{Pu}$	727.9	$1.24 \times 10^{-9}$	6
$^{239}\text{Pu}$	658.929	$9.69 \times 10^{-8}$	6	$^{241}\text{Am}$	729.52	$1.33 \times 10^{-8}$	6
$^{137}\text{Cs}$	661.635	$8.51 \times 10^{-1}$	7	<u>Group XIII</u> (753.5 - 773.5 keV)			
$^{241}\text{Am}$	662.420	$3.64 \times 10^{-6}$	6	$^{241}\text{Am}$	755.91	$7.60 \times 10^{-8}$	6
<u>Group XI</u> (684.0 - 711.5 keV)				$^{239}\text{Pu}$	756.40	$3.47 \times 10^{-8}$	6
$^{240}\text{Pu}$	687.7	$3.55 \times 10^{-8}$	6	$^{95}\text{Zr}$	756.72	$5.46 \times 10^{-1}$	7
$^{241}\text{Am}$	688.77	$3.25 \times 10^{-7}$	6	$^{241}\text{Am}$	759.46	$1.67 \times 10^{-8}$	6
$^{241}\text{Am}$	693.49	$3.68 \times 10^{-8}$	6	$^{228}\text{Th}$	763.34	$5.78 \times 10^{-3}$	7
$^{144}\text{Ce}$	696.4	$1.5 \times 10^{-2}$	7	$^{241}\text{Am}$	763.4	$1.96 \times 10^{-9}$	6
$^{241}\text{Am}$	696.44	$5.34 \times 10^{-8}$	6	$^{239}\text{Pu}$	763.7	$3.24 \times 10^{-10}$	6
$^{239}\text{Pu}$	701.1	$5.12 \times 10^{-9}$	6	$^{95}\text{Zr}$ - $^{95}\text{Nb}$	765.79	$9.9 \times 10^{-1}$	7
$^{239}\text{Pu}$	703.73	$3.95 \times 10^{-8}$	6	$^{238}\text{Pu}$	766.41	$2.19 \times 10^{-7}$	6
$^{241}\text{Am}$	709.41	$6.41 \times 10^{-8}$	6	$^{239}\text{Pu}$	766.6	$2.75 \times 10^{-9}$	6
<u>Group XII</u> (716.0 - 732.0 keV)				$^{241}\text{Am}$	766.92	$5.00 \times 10^{-8}$	6
$^{239}\text{Pu}$	717.72	$2.74 \times 10^{-8}$	6	$^{239}\text{Pu}$	769.37	$1.12 \times 10^{-7}$	6
$^{239}\text{Pu}$	720.3	$4.85 \times 10^{-10}$	6	$^{241}\text{Am}$	770.58	$4.74 \times 10^{-8}$	6
$^{241}\text{Am}$	721.990	$1.96 \times 10^{-6}$	6	$^{241}\text{Am}$	772.13	$2.66 \times 10^{-8}$	6
$^{95}\text{Zr}$	724.18	$4.3 \times 10^{-1}$	7	<u>Group XIV</u> (735.0 - 745.0 keV)			
$^{228}\text{Th}$	727.28	$6.36 \times 10^{-2}$	7	$^{241}\text{Am}$	737.29	$8.00 \times 10^{-8}$	6

Table 1. (continued)

Source	Energy (keV)	Intensity	Reference	Source	Energy (keV)	Intensity	Reference
$^{238}\text{Pu}$	742.82	$5.17 \times 10^{-8}$	6				

Table 2. Comparison of the present results with mass-spectrometric data.

	$^{238}\text{Pu}$	$^{239}\text{Pu}$	$^{240}\text{Pu}$	$^{241}\text{Pu}$
1	$0.036 \pm 0.012$	$91.5 \pm 0.6$	$7.9 \pm 0.7$	$0.560 \pm 0.010$
2	$0.027 \pm 0.013$	$91.5 \pm 0.7$	$7.9 \pm 0.8$	$0.549 \pm 0.011$
3	$0.034 \pm 0.017$	$91.7 \pm 1.0$	$7.7 \pm 1.2$	$0.541 \pm 0.016$
4	$0.023 \pm 0.014$	$91.1 \pm 0.7$	$8.1 \pm 0.9$	$0.549 \pm 0.012$
Average	$0.030 \pm 0.004$	$91.5 \pm 0.2$	$7.9 \pm 0.1$	$0.550 \pm 0.005$
MS data	0.033	91.216	7.966	0.610

## Figure Captions

Fig.1. A schematic view of the counting set-up for the non-destructive analysis of plutonium.

Fig.2. A typical example of the obtained  $\gamma$ -ray spectrum. The channel number in the abscissa corresponds to four times the energy.

Fig.3. Illustration of the prominent peaks used for the energy calibration which are designated with arrows, and the peak groupings unfolded for determination of the isotopic ratios of plutonium. The groupings coloured in red were of particular importance in the isotopic ratio determination.

Fig.4. Results of the unfolding of the group IV; a) 92% and b) 75% with respect to  $^{239}\text{Pu}$ , respectively. The background continuum is depicted with dotted line. The  $\gamma$ -ray spectrum to be attributed to each nuclide involved is presented with a coloured line, respectively. Sum of the three response profiles and the background continuum makes the synthesized spectrum given with the black solid line, while observed data after being smoothed are plotted with circles.

Fig.5. Results of the unfolding of the group V; a) 92% and b) 75% with respect to  $^{239}\text{Pu}$ , respectively. For detailed

explanation, see the caption of Fig.4.

Fig.6. Results of the unfolding of the group VI; a) 92% and b) 75% with respect to  $^{239}\text{Pu}$ , respectively. Only two nuclides,  $^{239}\text{Pu}$  and  $^{241}\text{Am}$ , are involved in this grouping instead of three. For detailed explanation, see the caption of Fig.4.

Fig.7. Results of the unfolding of the group IX; a) 92% and b) 75% with respect to  $^{239}\text{Pu}$ , respectively. This grouping supplies the information for the  $^{240}\text{Pu}/^{239}\text{Pu}$  ratio. For further explanation, see the caption of Fig.4.

Fig.8. Results of the unfolding of the group XI; a) 92% and b) 75% with respect to  $^{239}\text{Pu}$ , respectively. This grouping also gives the information on the  $^{240}\text{Pu}/^{239}\text{Pu}$  ratio, though the reliability is generally poorer than that with the group IX. For further explanation, see the caption of Fig.4.

Fig.9. Results of the unfolding of the group XII; a), b), and c) 92%  $^{239}\text{Pu}$  samples with contamination of different amounts of  $^{95}\text{Zr}$ , and d) 75%  $^{239}\text{Pu}$  sample. One can deduce the  $^{228}\text{Th}/^{239}\text{Pu}$  ratio with this grouping. For further explanation, see the caption of Fig.4.

Fig.10. Results of the unfolding of the group XIII; a), b), and c) 92%  $^{239}\text{Pu}$  samples with contamination of different

amounts of  $^{95}\text{Zr}$ - $^{95}\text{Nb}$ , and d) 75%  $^{239}\text{Pu}$  sample. Information on the  $^{238}\text{Pu}/^{239}\text{Pu}$  and the  $^{228}\text{Th}/^{239}\text{Pu}$  ratio is obtainable with this grouping. For further explanation, see the caption of Fig.4.

Fig.11. Results of the unfolding of the group XIV; 75% and 92% with respect to the  $^{239}\text{Pu}$  content, respectively. This doublet supplies information on the  $^{238}\text{Pu}/^{239}\text{Pu}$  ratio by the use of the known value of the  $^{241}\text{Am}/^{239}\text{Pu}$  ratio. For further explanation, see the caption of Fig.4.

Fig.12. Results of the unfolding of the group II; 75% and 92% with respect to the  $^{239}\text{Pu}$  content, respectively. For further explanation, see the caption of Fig.4.

Fig.13. Results of the unfolding of the group VIII; a), b), and c) 92%  $^{239}\text{Pu}$  sample with contamination of different amounts of  $^{106}\text{Ru}$ , and d) 75%  $^{239}\text{Pu}$  sample. For further explanation, see the caption of Fig.4.

Fig.14. Results of the unfolding of the group X; a) 92% and 75% with respect to the  $^{239}\text{Pu}$  content, respectively. For further explanation, see the caption of Fig.4.

Fig.15. An example of the relative detection efficiency curve constructed with twelve values of ~~of~~  $^{239}\text{Pu}$  intensity deduced in the unfolding of the peak groupings.



Fig.16. Comparison between the observed (filled circles with error bar) and the book (open circles) value for the content of fissile plutonium. Sixty-three spectrum data subjected to the test were taken with plutonium samples of three grades; namely, a) 92%, b) 81%, and c) 75% with respect to the fissile plutonium, respectively.

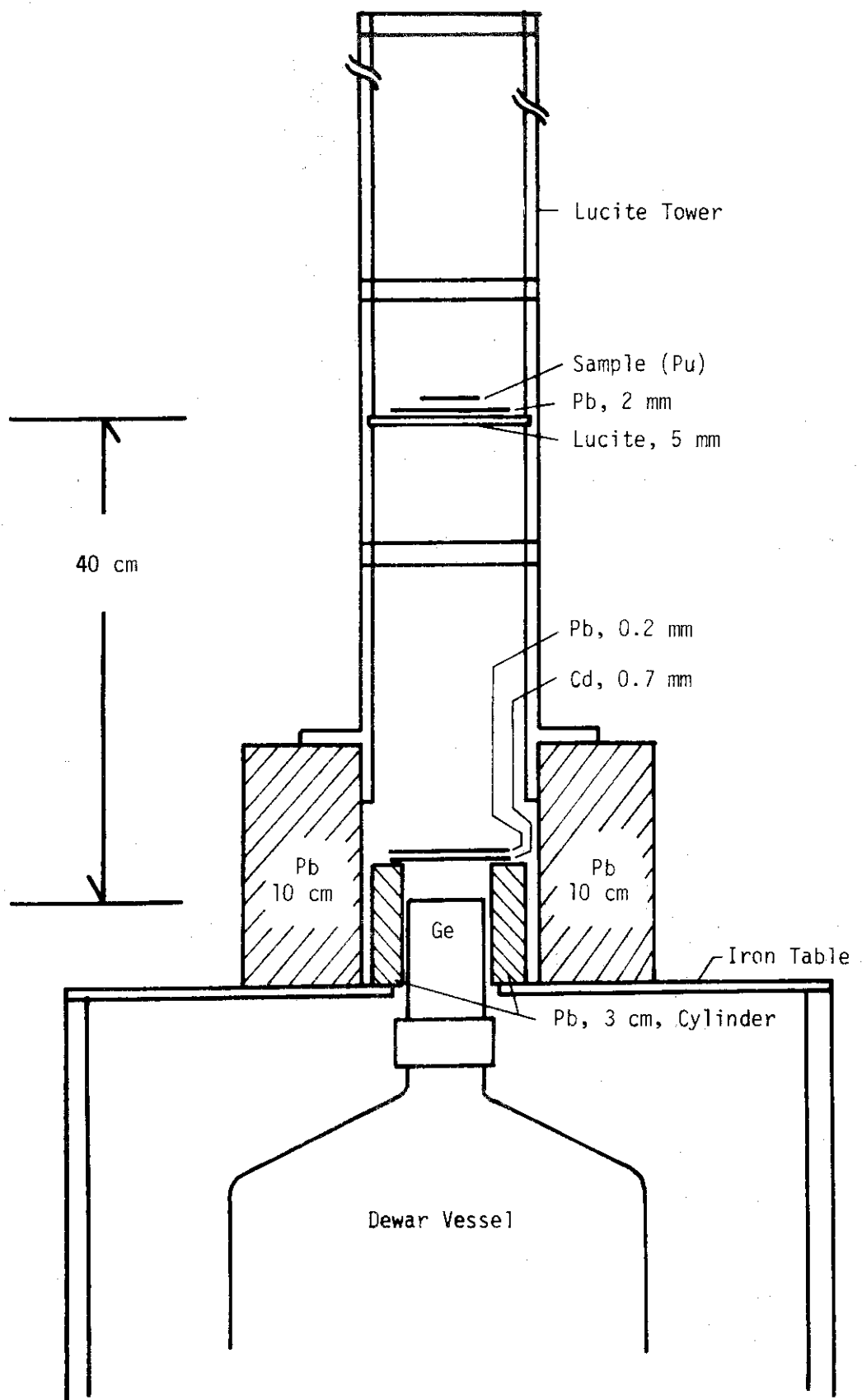


Fig.1. A schematic view of the counting set-up for the non-destructive analysis of plutonium.



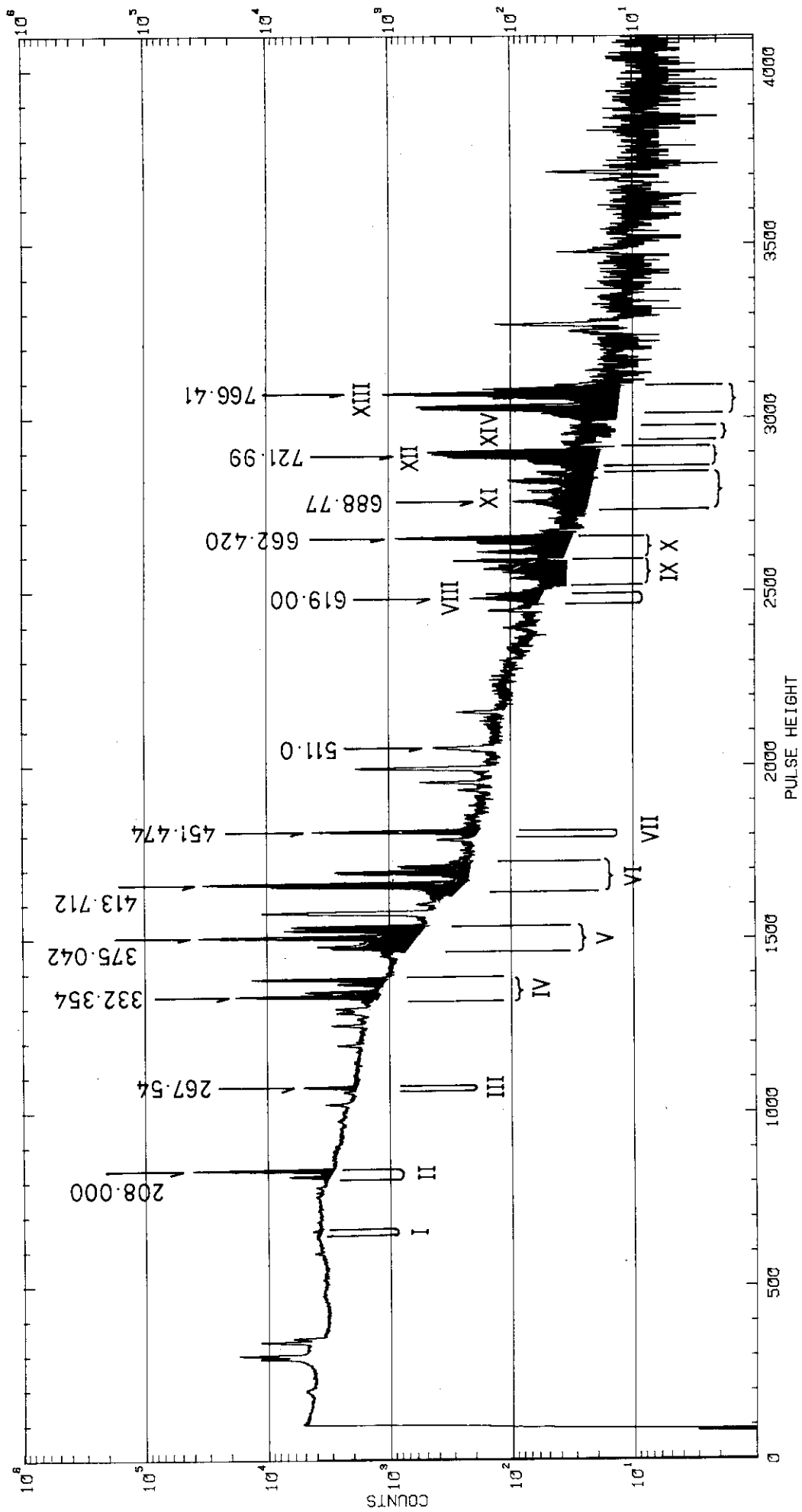


Fig. 3

Fig. 4a

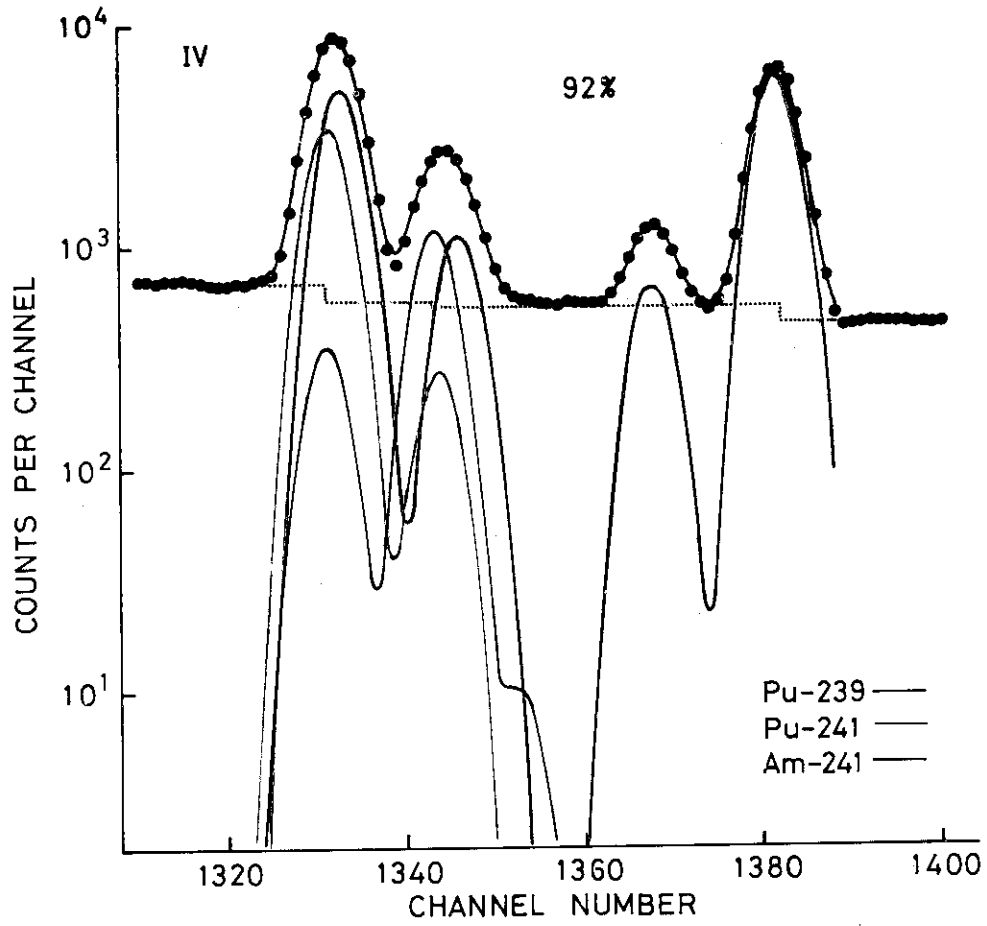


Fig. 4b

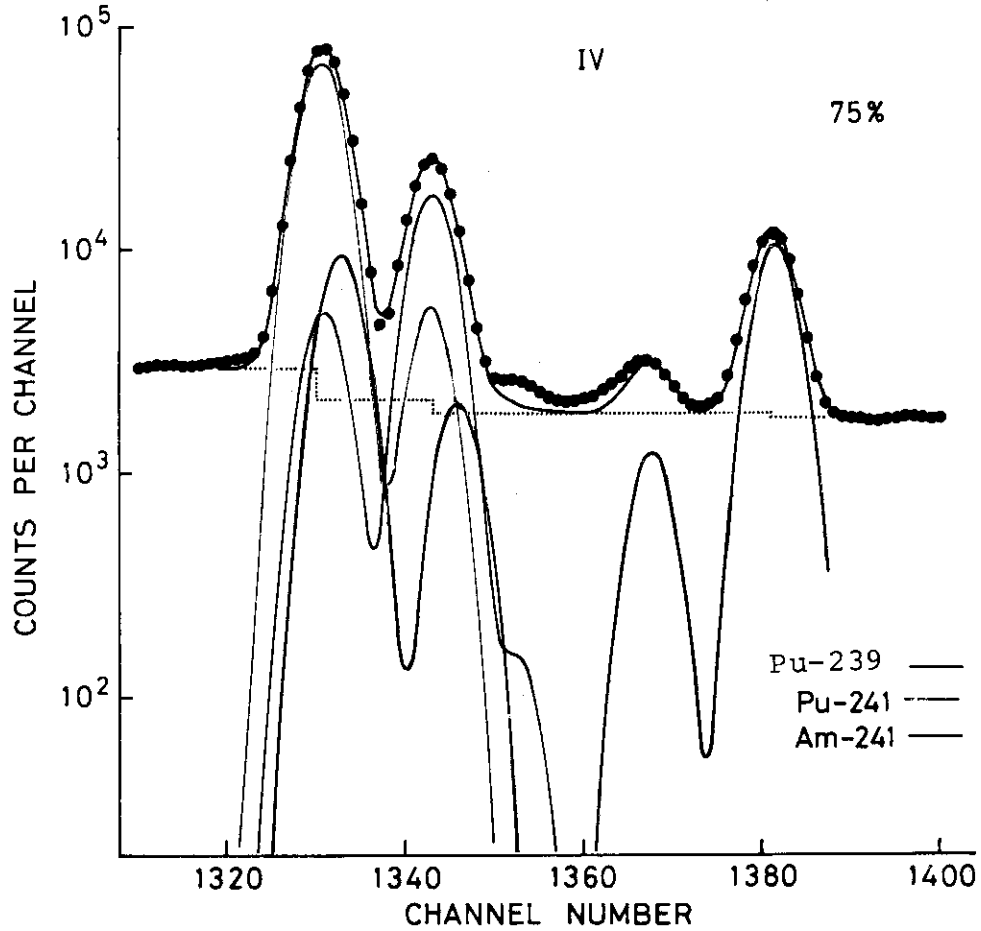


Fig. 5a

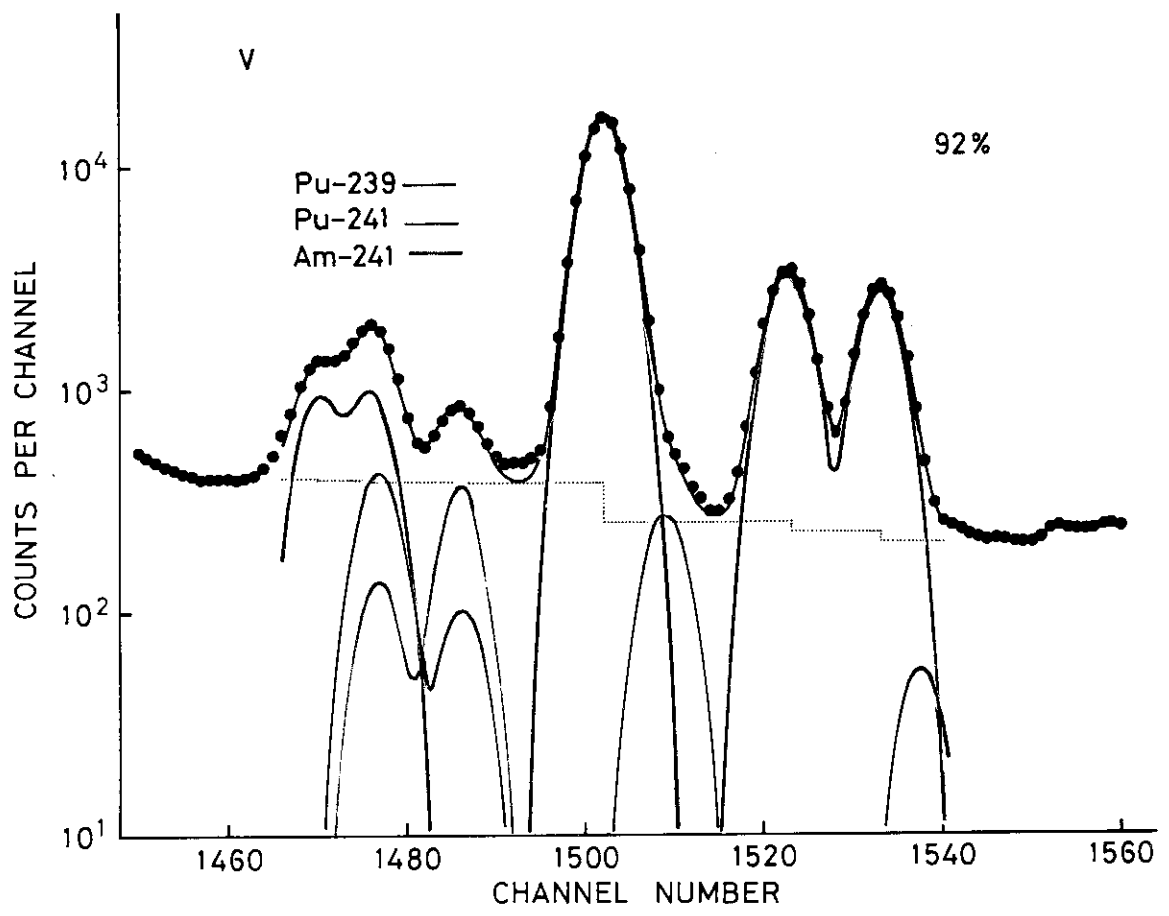


Fig. 5b

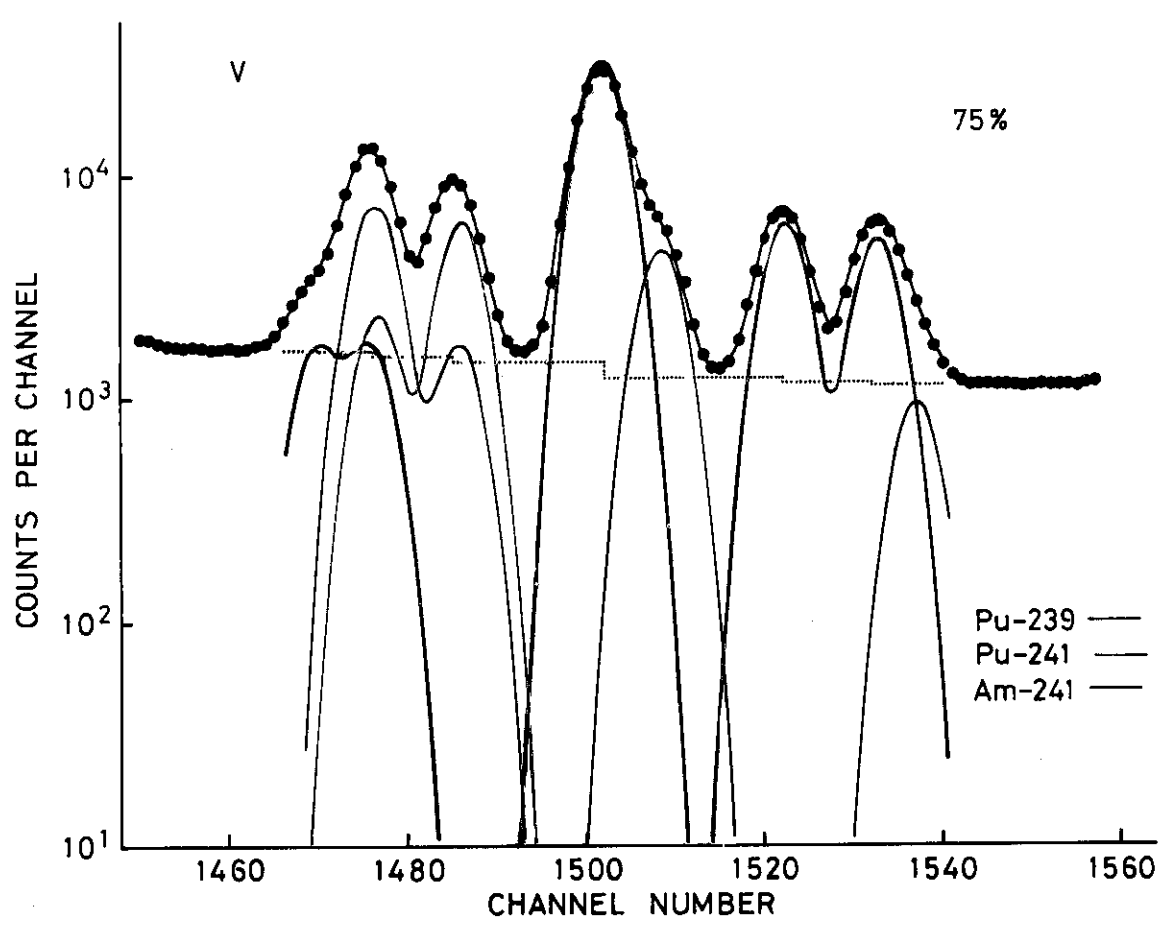


Fig. 6a

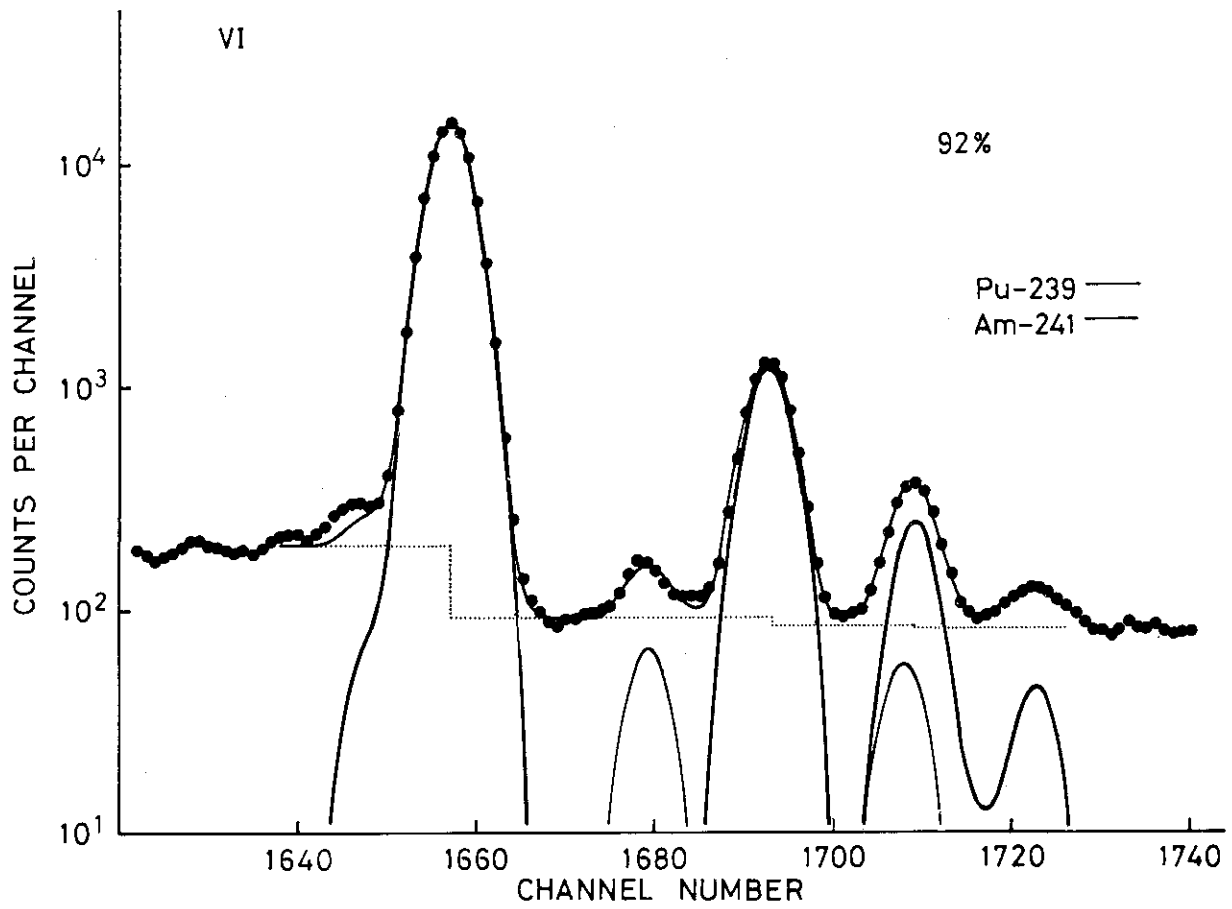
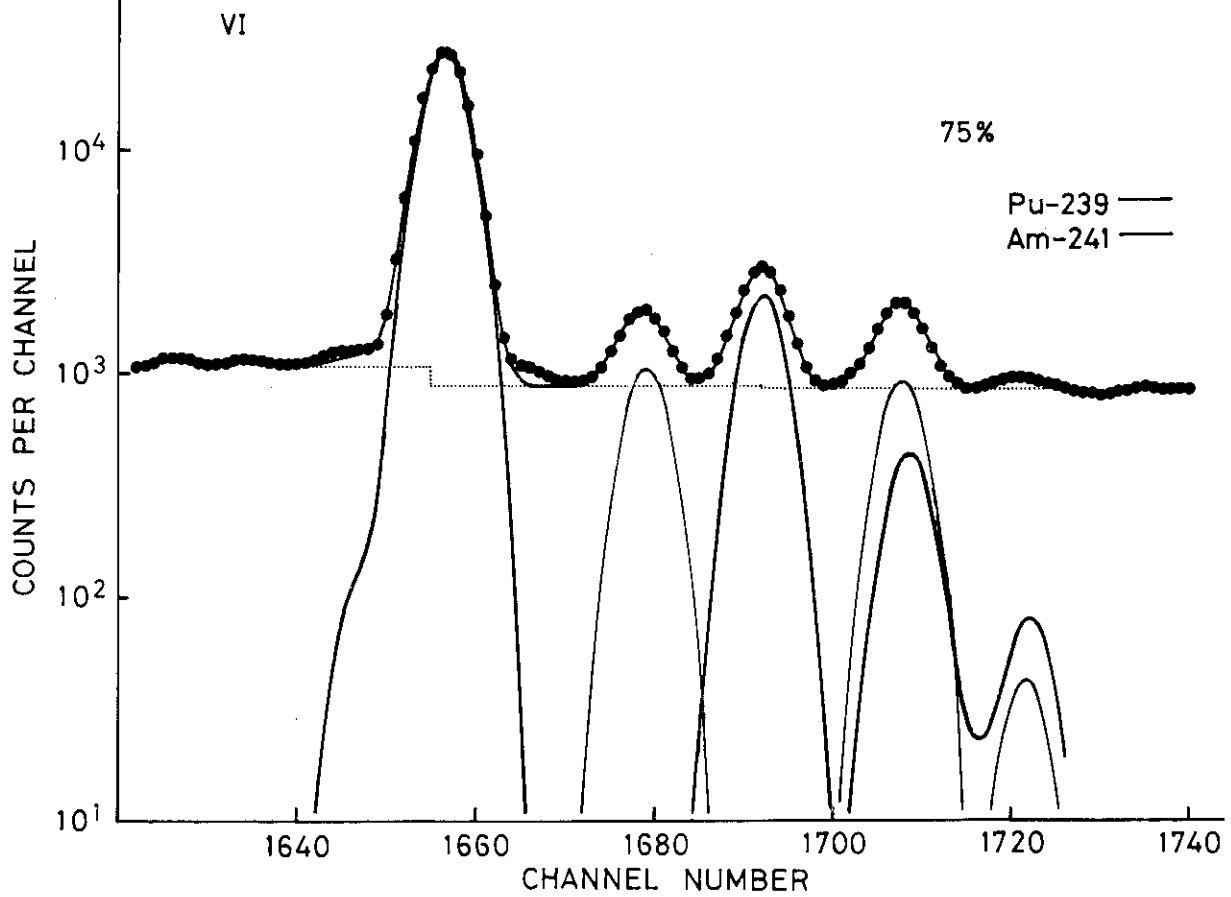


Fig. 6b



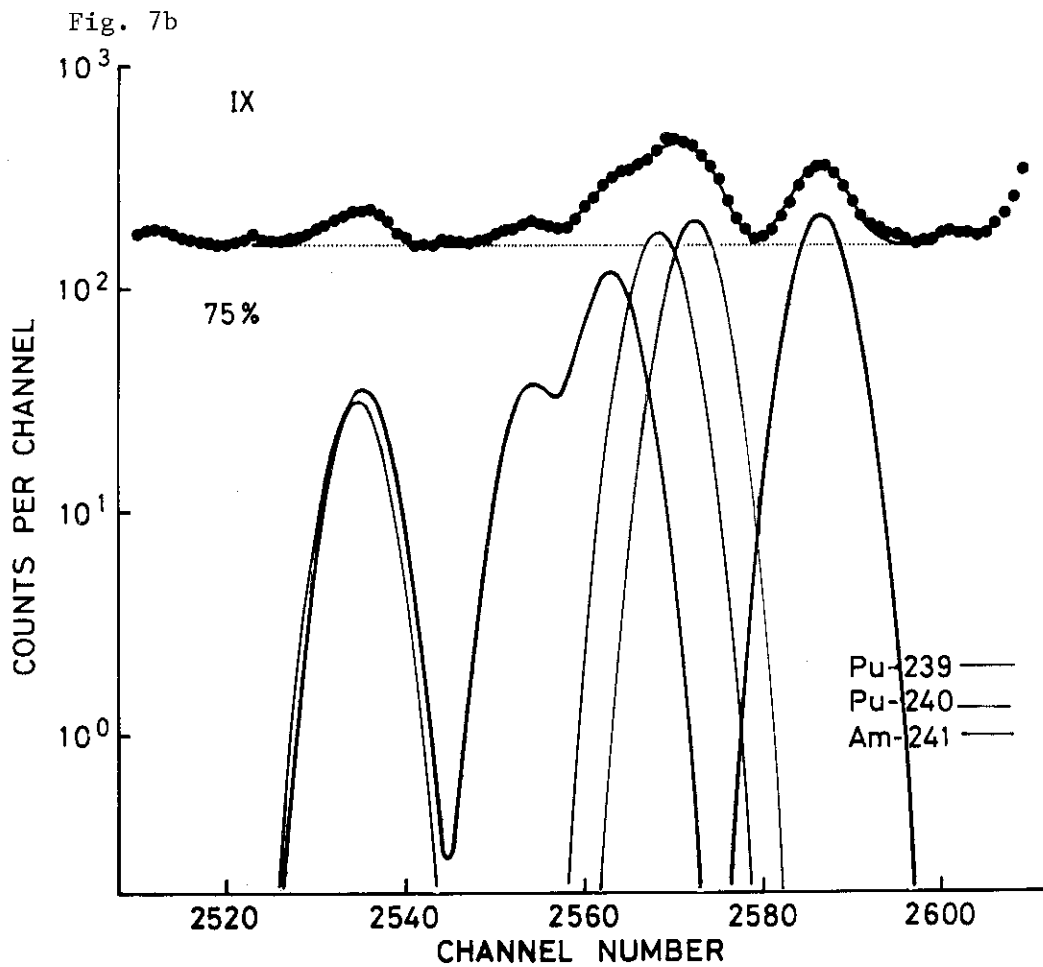
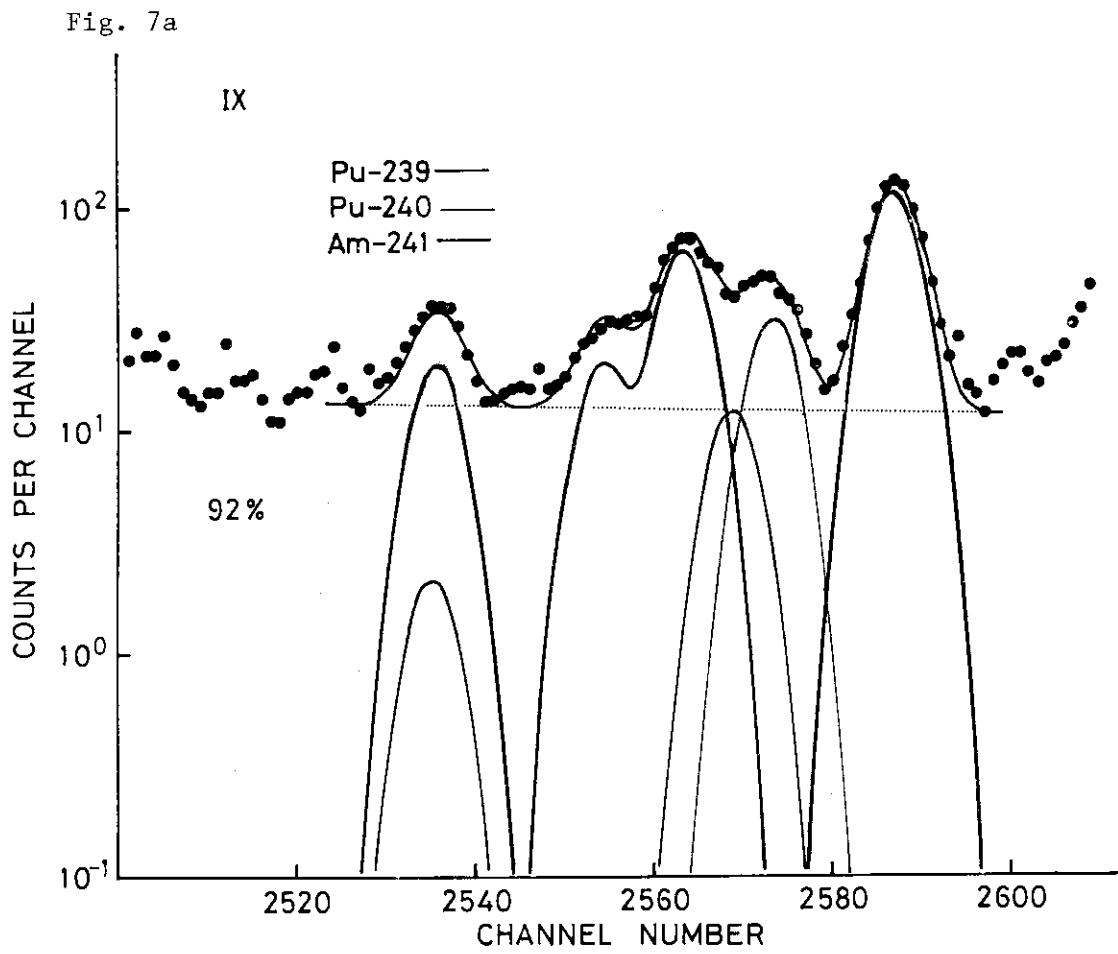




Fig. 8a

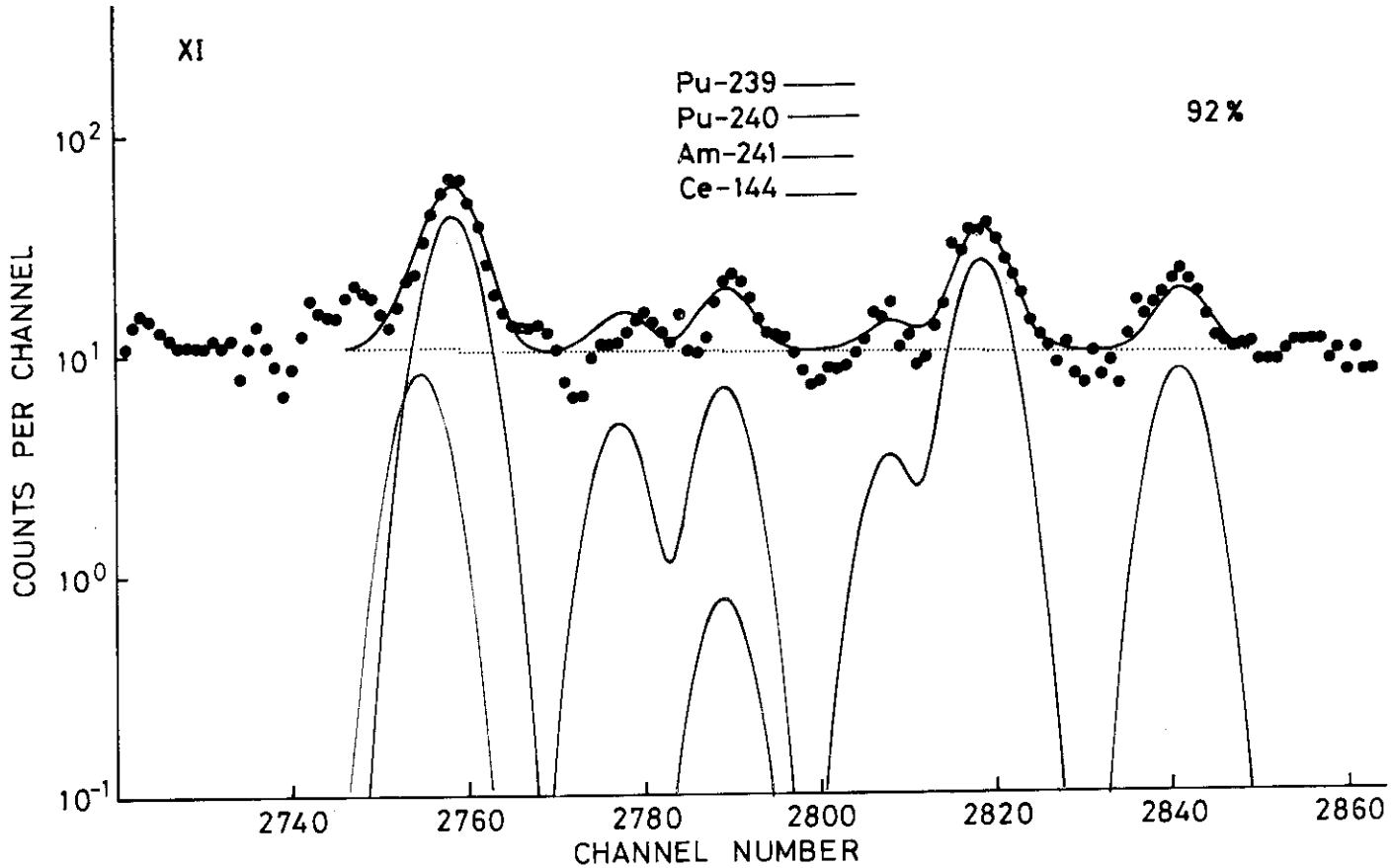


Fig. 8b

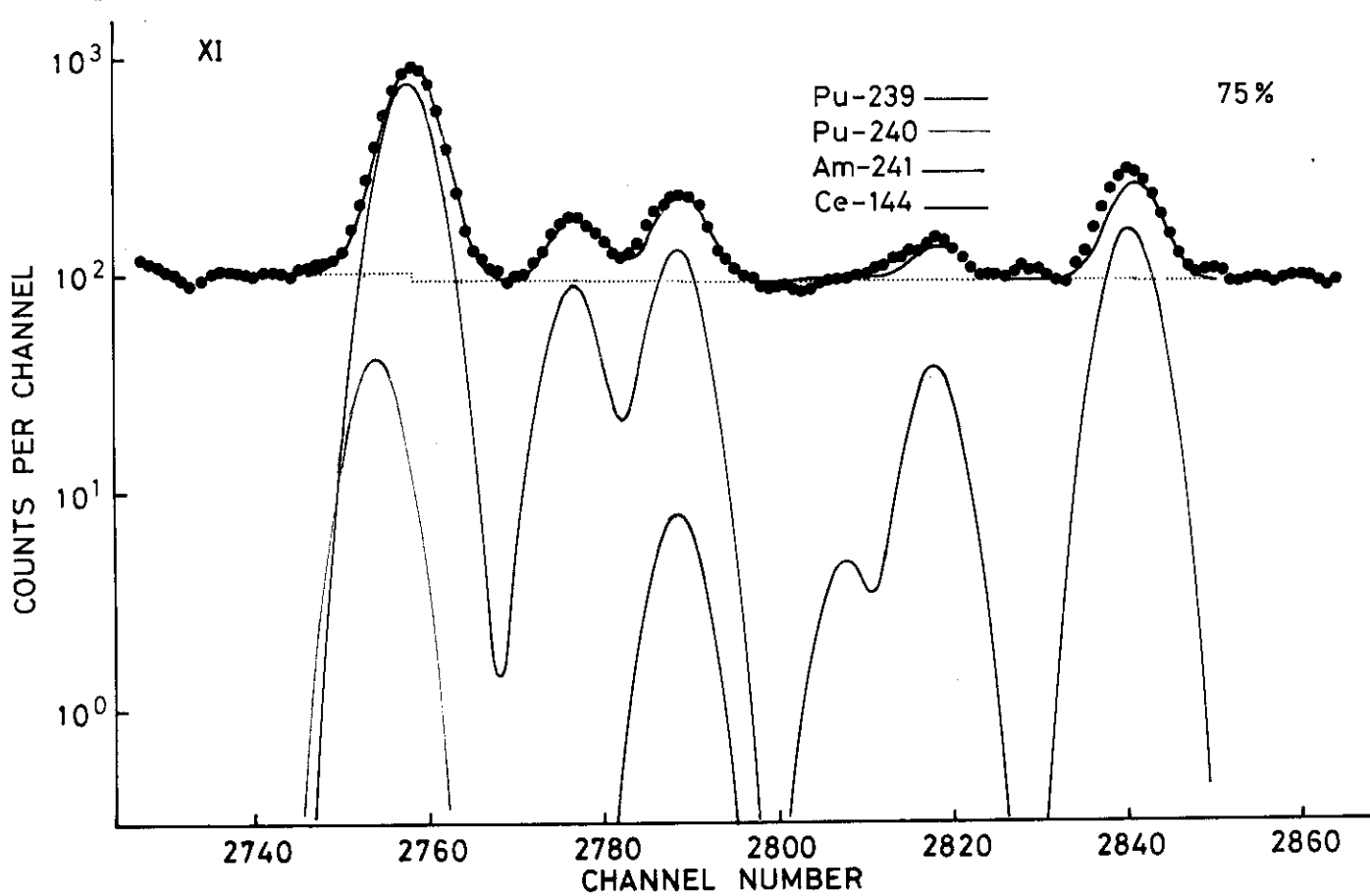


Fig. 9a

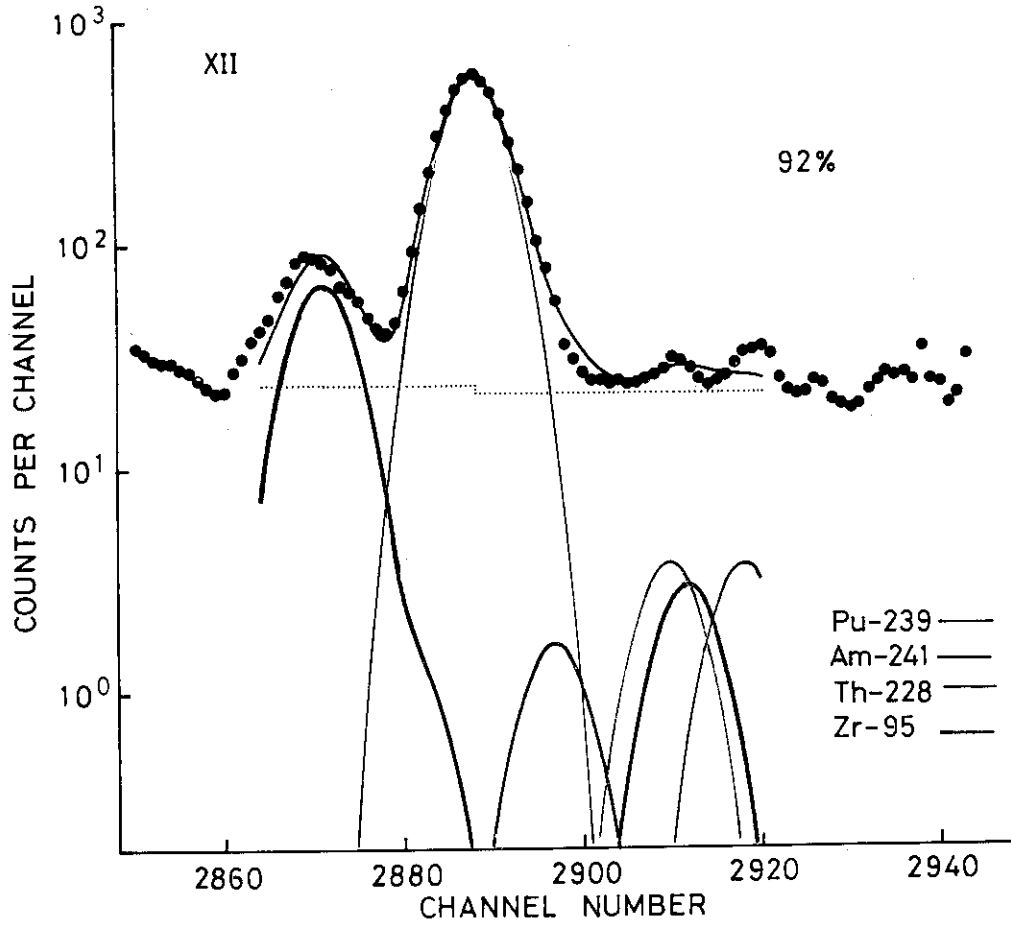


Fig. 9b

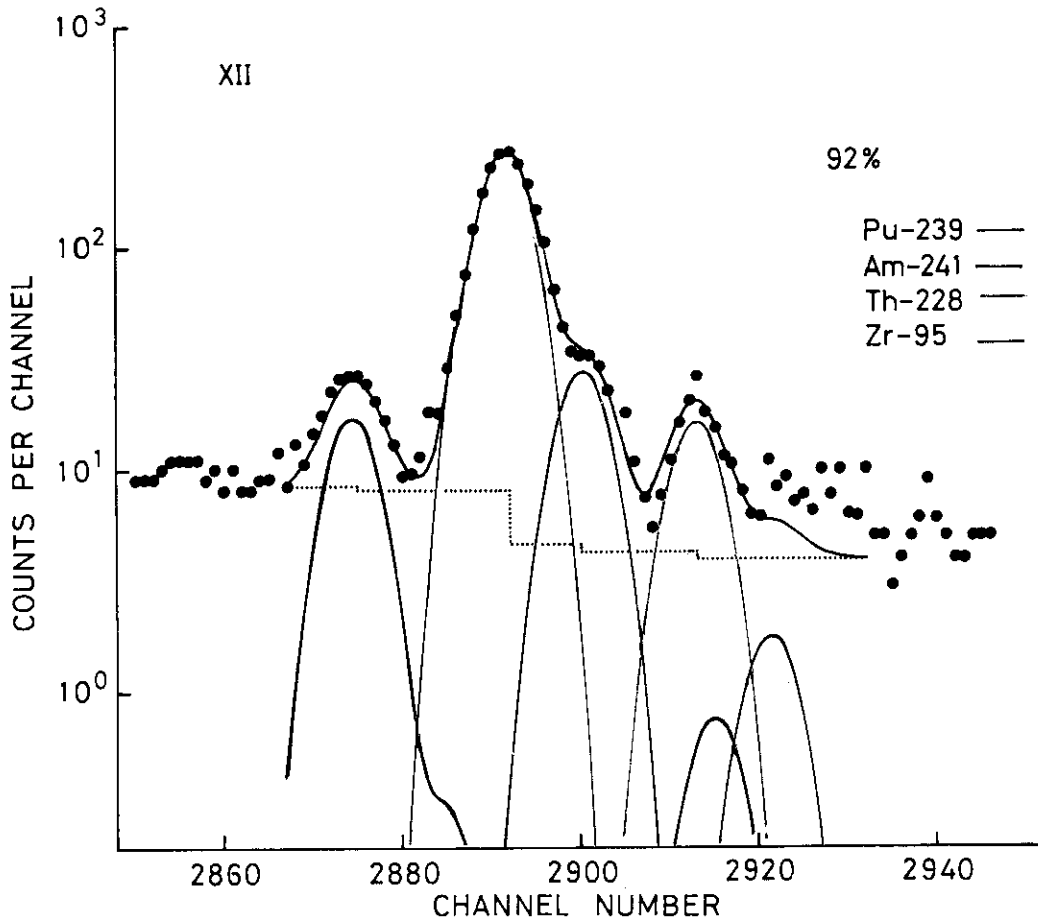


Fig. 9c

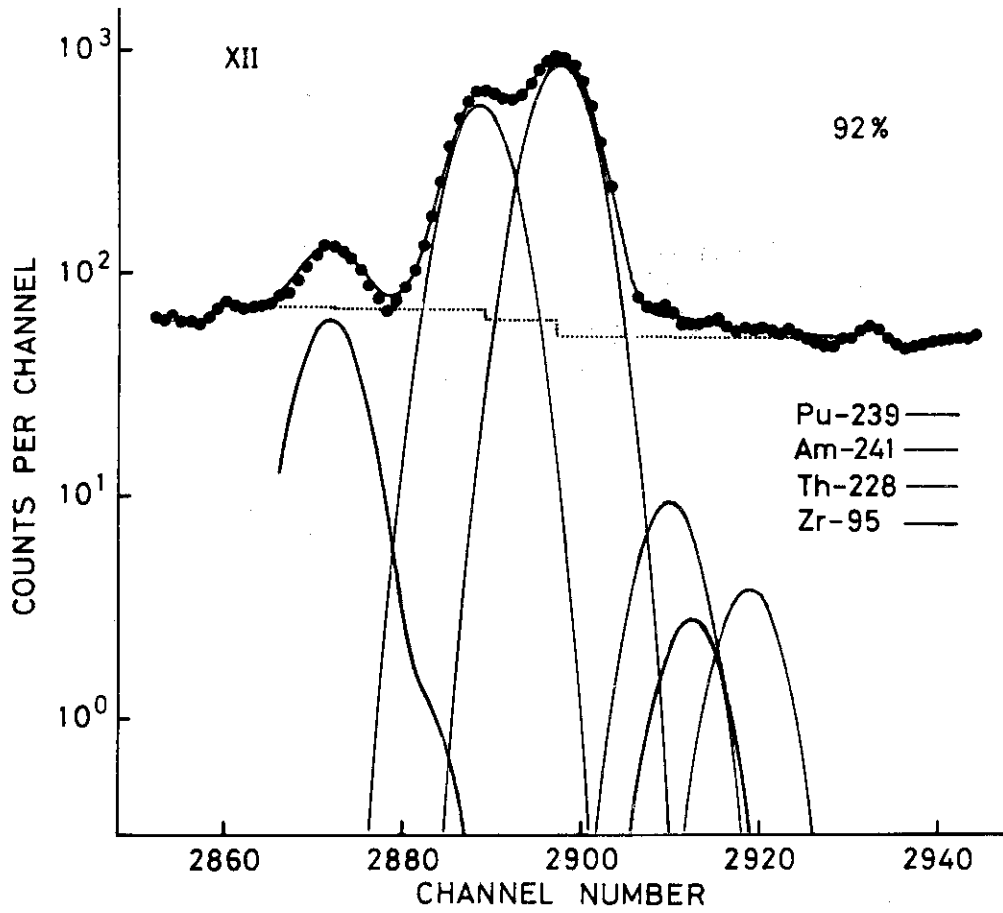


Fig. 9d

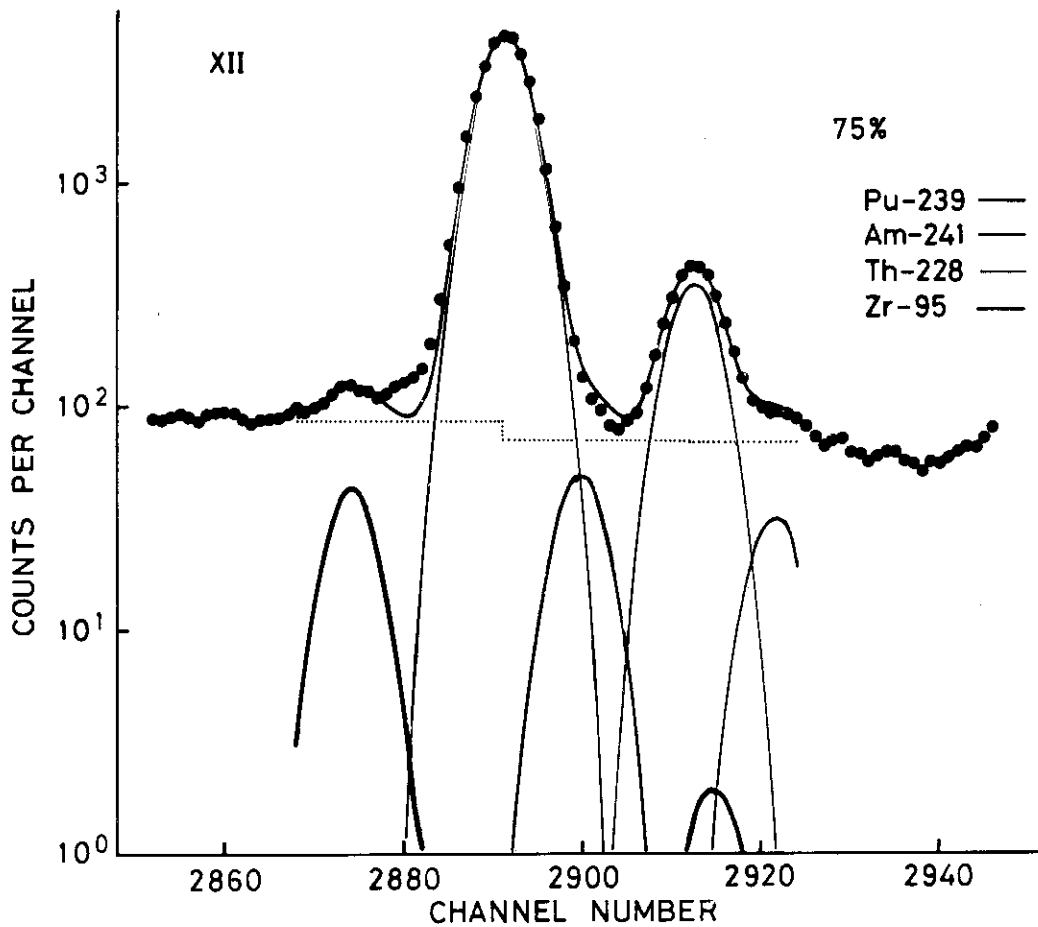


Fig. 10a

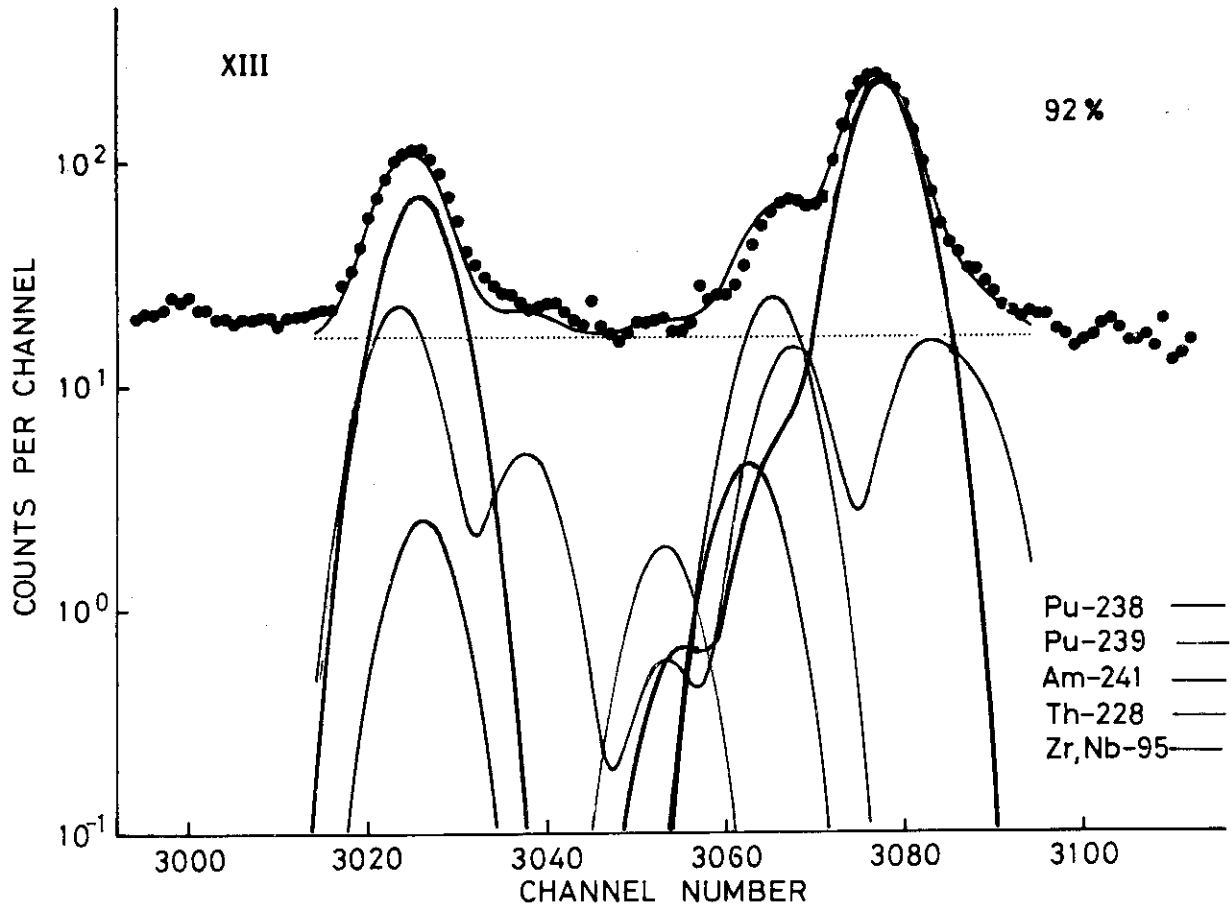


Fig. 10b

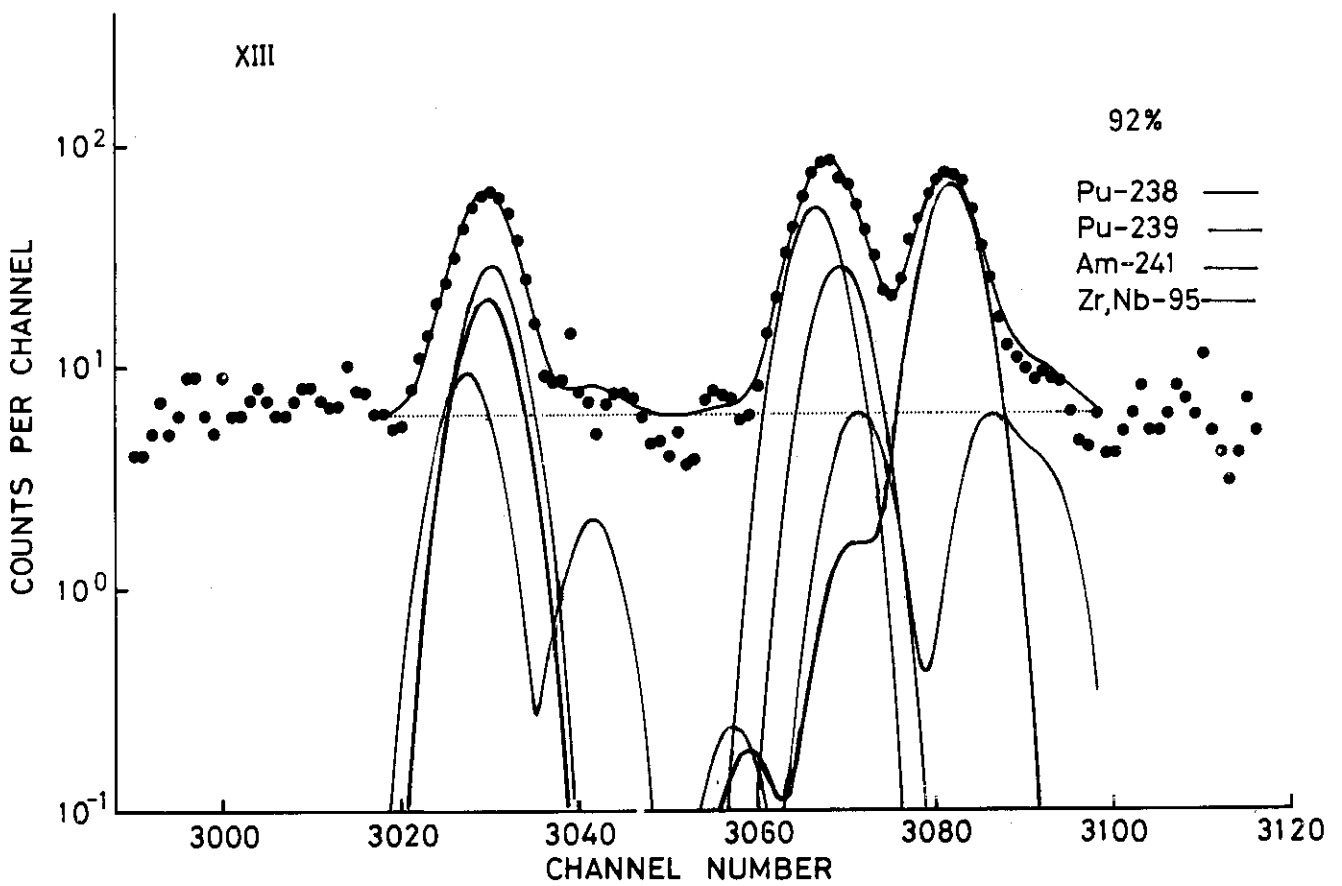


Fig. 10c

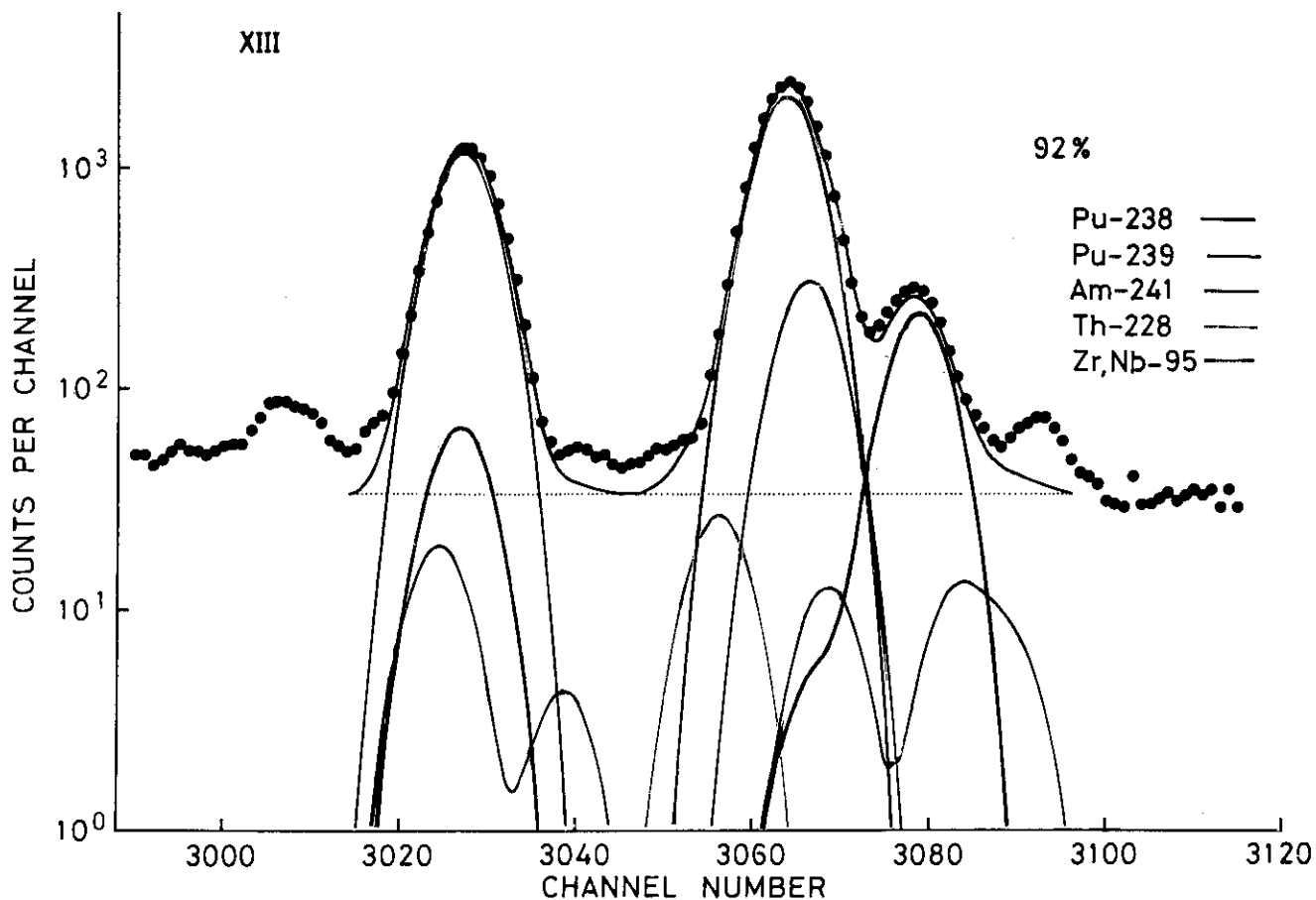


Fig. 10d

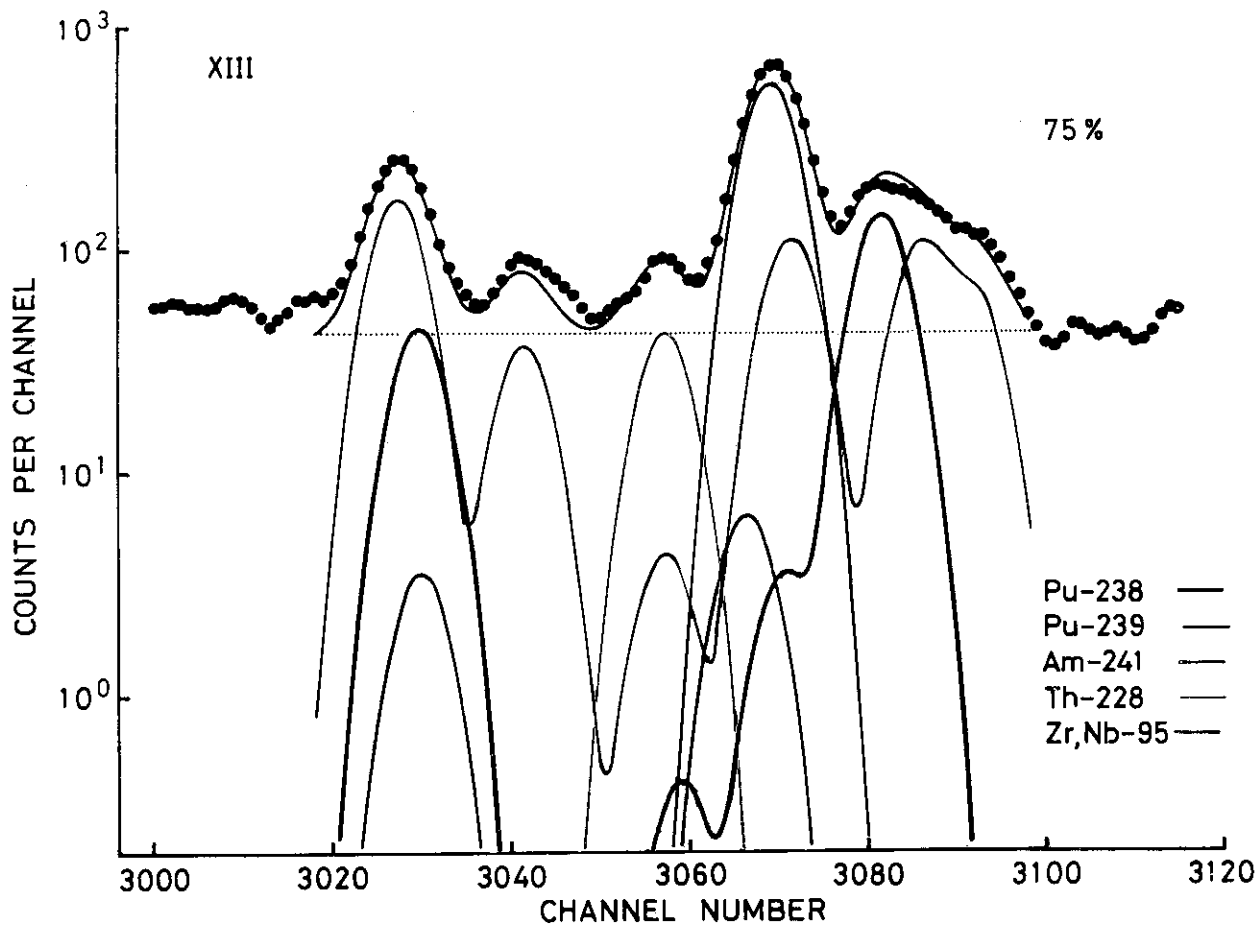


Fig. 11

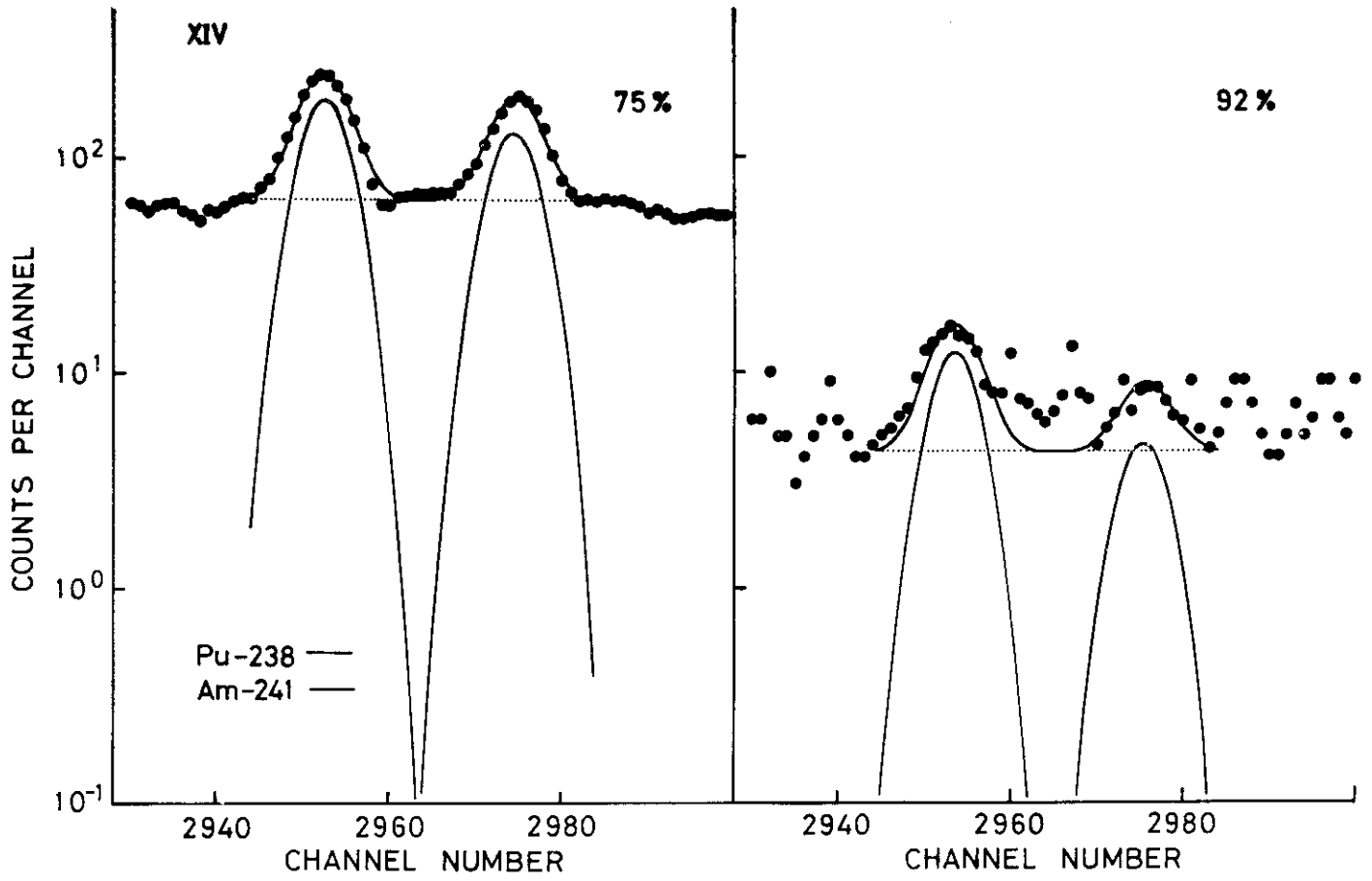
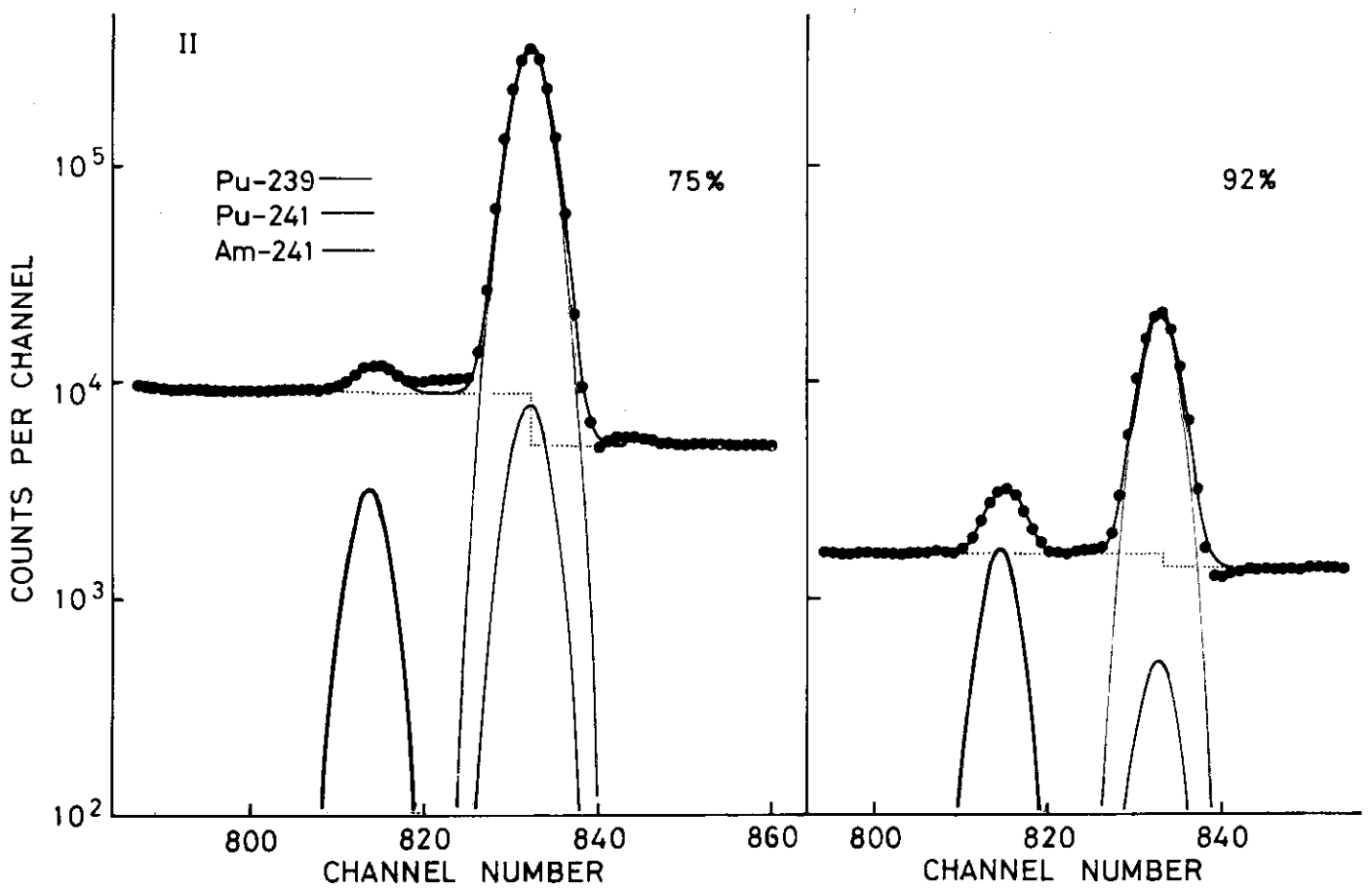


Fig. 12



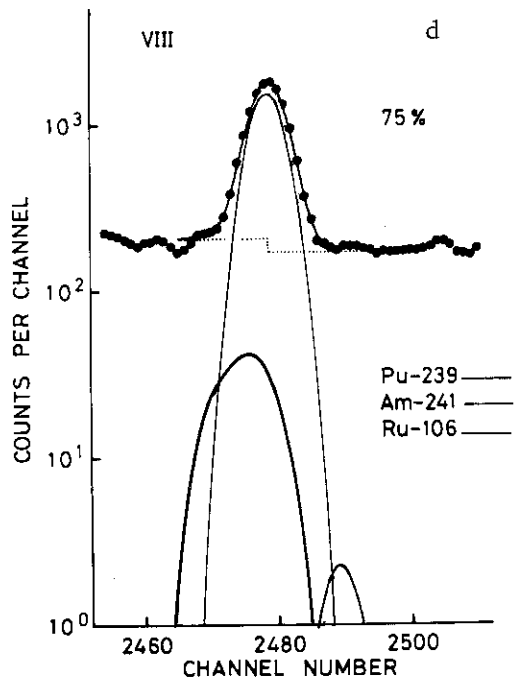
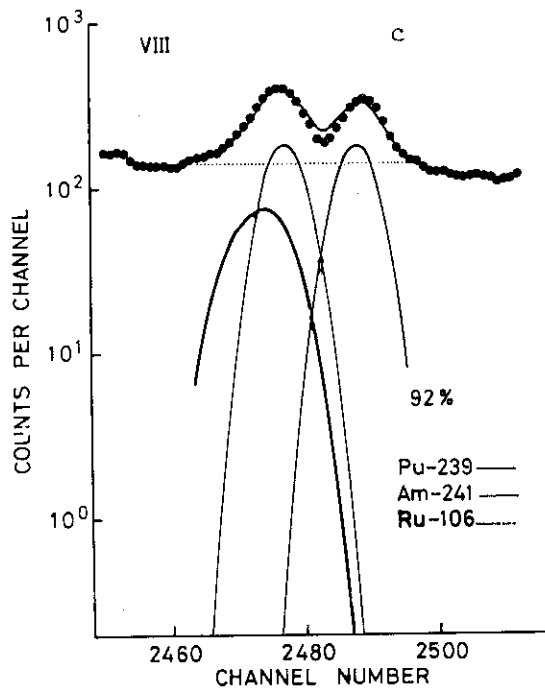
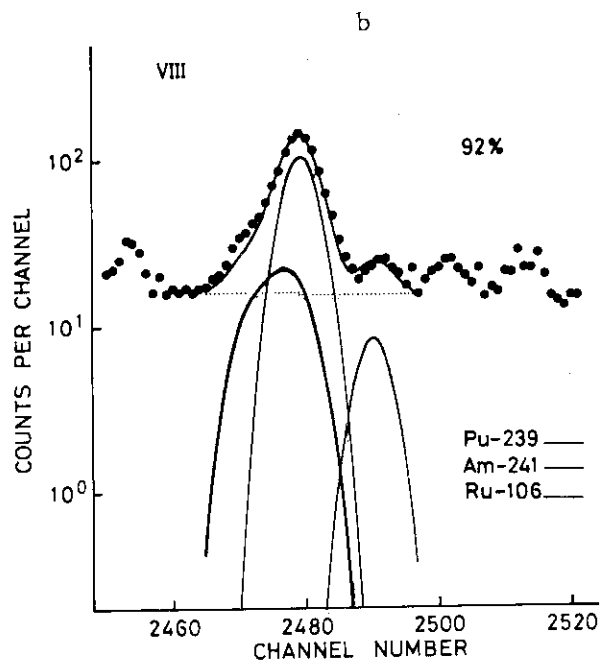
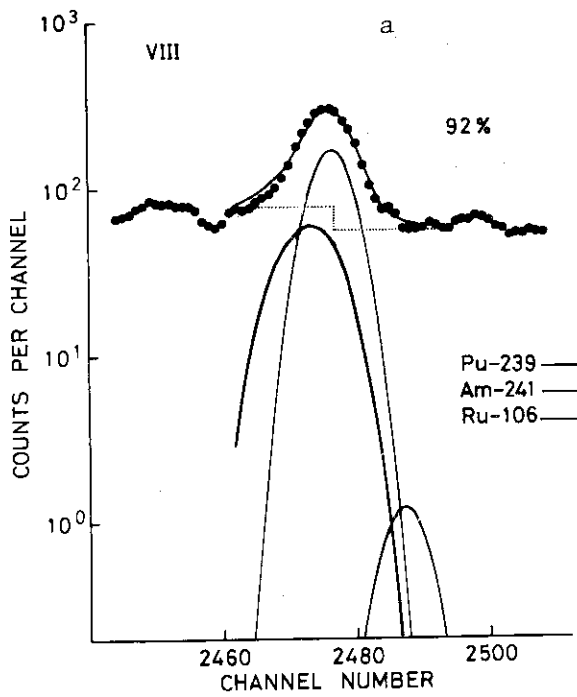


Fig. 13

Fig. 14a

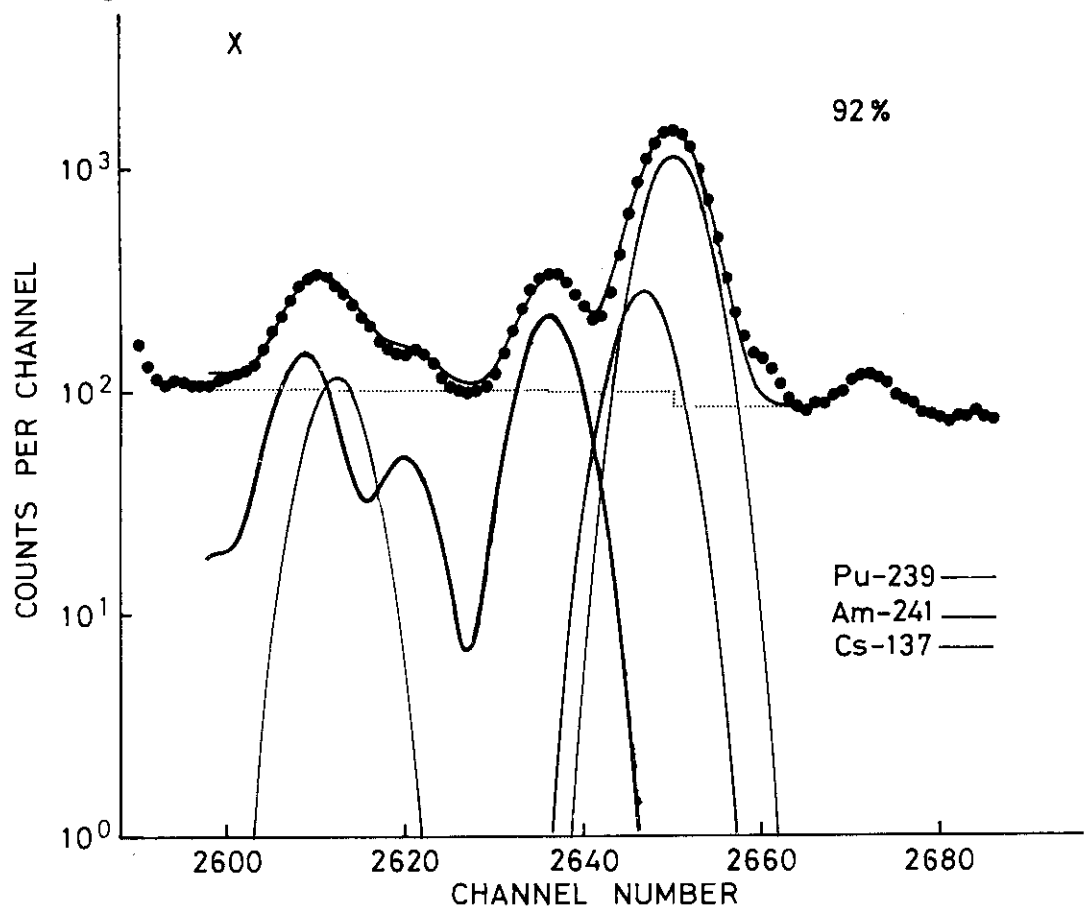
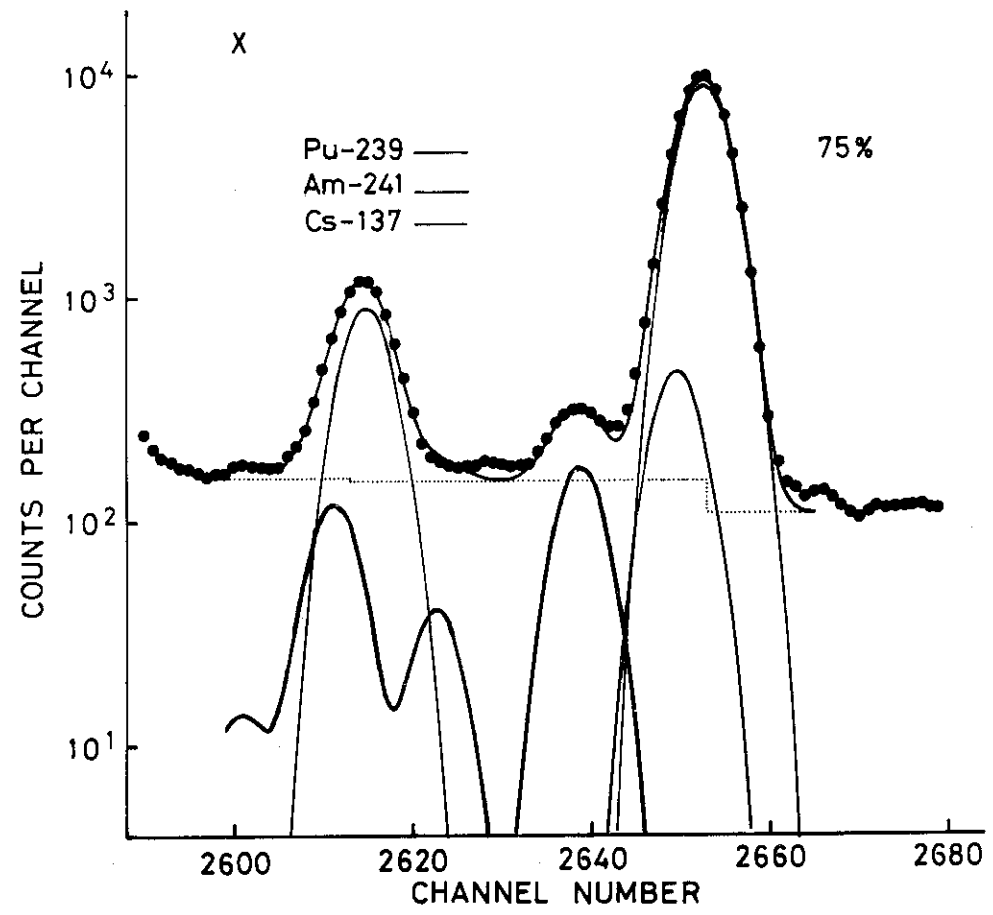


Fig. 14b





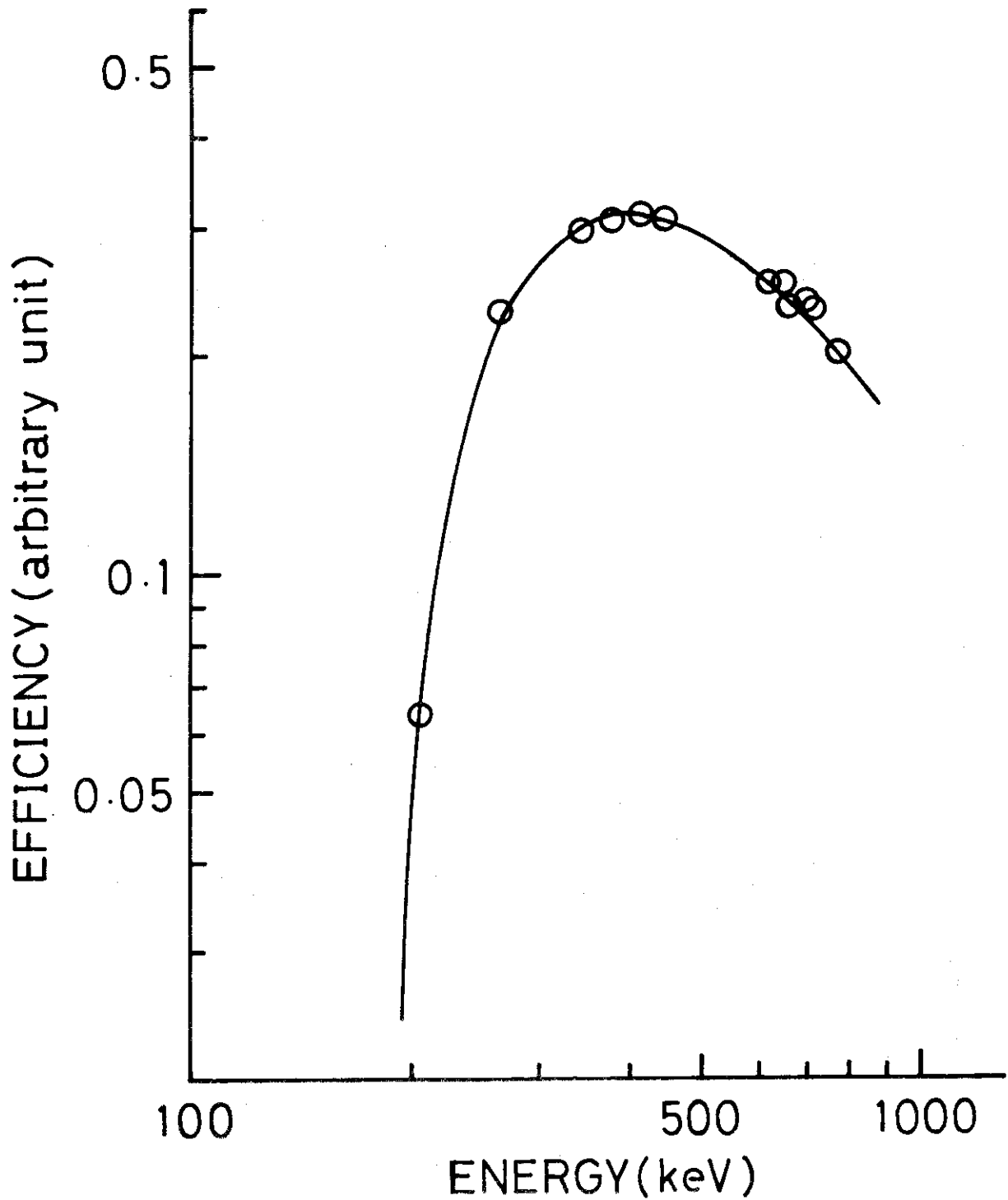


Fig.15. An example of the relative detection efficiency curve constructed with twelve values of  $\epsilon_{\beta}$  of  $^{239}\text{Pu}$  intensity deduced in the unfolding of the peak groupings.

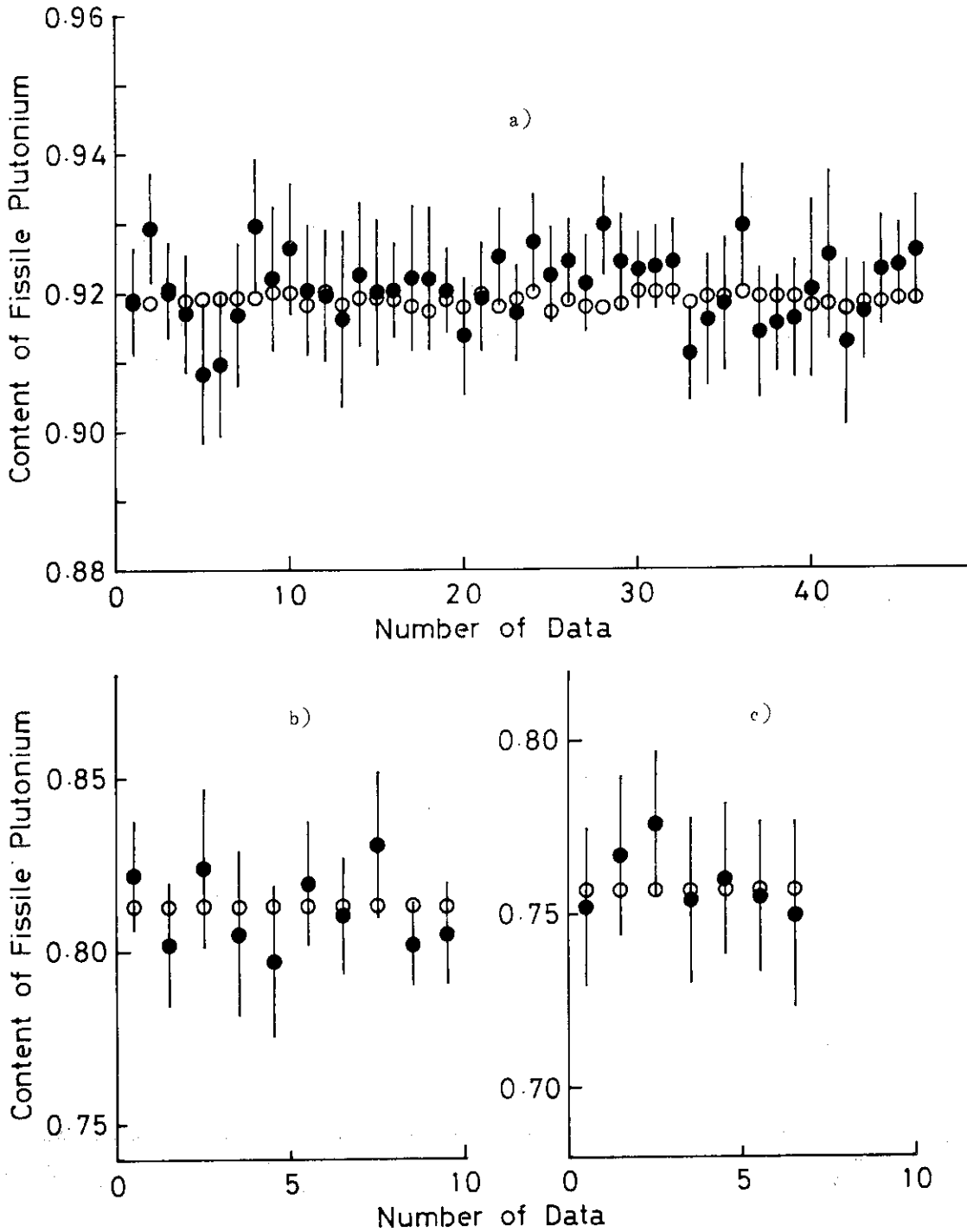


Fig.16. Comparison between the observed (filled circles with error bar) and the book (open circles) value for the content of fissile plutonium. Sixty-three spectrum data subjected to the test were taken with plutonium samples of three grades; namely, a) 92%, b) 81%, and c) 75% with respect to the fissile plutonium, respectively.